

Spring 1988

Ab initio molecular orbital investigations of molecular structures for lithiated hydrocarbons

Shu-Jun Su

University of New Hampshire, Durham

Follow this and additional works at: <https://scholars.unh.edu/dissertation>

Recommended Citation

Su, Shu-Jun, "Ab initio molecular orbital investigations of molecular structures for lithiated hydrocarbons" (1988). *Doctoral Dissertations*. 1547.

<https://scholars.unh.edu/dissertation/1547>

This Dissertation is brought to you for free and open access by the Student Scholarship at University of New Hampshire Scholars' Repository. It has been accepted for inclusion in Doctoral Dissertations by an authorized administrator of University of New Hampshire Scholars' Repository. For more information, please contact nicole.hentz@unh.edu.

INFORMATION TO USERS

The most advanced technology has been used to photograph and reproduce this manuscript from the microfilm master. UMI films the original text directly from the copy submitted. Thus, some dissertation copies are in typewriter face, while others may be from a computer printer.

In the unlikely event that the author did not send UMI a complete manuscript and there are missing pages, these will be noted. Also, if unauthorized copyrighted material had to be removed, a note will indicate the deletion.

Oversize materials (e.g., maps, drawings, charts) are reproduced by sectioning the original, beginning at the upper left-hand corner and continuing from left to right in equal sections with small overlaps. Each oversize page is available as one exposure on a standard 35 mm slide or as a 17" x 23" black and white photographic print for an additional charge.

Photographs included in the original manuscript have been reproduced xerographically in this copy. 35 mm slides or 6" x 9" black and white photographic prints are available for any photographs or illustrations appearing in this copy for an additional charge. Contact UMI directly to order.



300 North Zeeb Road, Ann Arbor, MI 48106-1346 USA

Order Number 8816702

***Ab initio* molecular orbital investigations of molecular structures
for lithiated hydrocarbons**

Su, Shu-Jun, Ph.D.

University of New Hampshire, 1988

U·M·I
300 N. Zeeb Rd.
Ann Arbor, MI 48106

PLEASE NOTE:

In all cases this material has been filmed in the best possible way from the available copy. Problems encountered with this document have been identified here with a check mark .

1. Glossy photographs or pages _____
2. Colored illustrations, paper or print _____
3. Photographs with dark background _____
4. Illustrations are poor copy _____
5. Pages with black marks, not original copy _____
6. Print shows through as there is text on both sides of page _____
7. Indistinct, broken or small print on several pages
8. Print exceeds margin requirements _____
9. Tightly bound copy with print lost in spine _____
10. Computer printout pages with indistinct print _____
11. Page(s) _____ lacking when material received, and not available from school or author.
12. Page(s) 65 seem to be missing in numbering only as text follows.
13. Two pages numbered 66. Text follows.
14. Curling and wrinkled pages _____
15. Dissertation contains pages with print at a slant, filmed as received
16. Other _____

U·M·I

***AB INITIO* MOLECULAR ORBITAL INVESTIGATIONS
OF MOLECULAR STRUCTURES FOR LITHIATED HYDROCARBONS**

By

Shu-Jun Su
M.S., Beijing Normal University, 1981

DISSERTATION

submitted to the University of New Hampshire
in partial fulfillment of
the Requirements for the Degree of

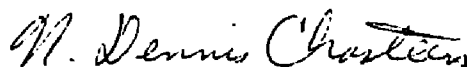
Doctor of Philosophy
in
Chemistry

May, 1988


This dissertation has been examined and approved.



Dissertation Director, Frank L. Pilar
(Professor of Chemistry)



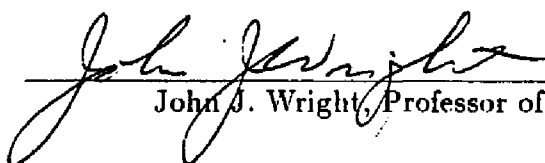
N. Dennis Chasteen, Professor of Chemistry



Howard R. Mayne, Assistant Professor of Chemistry



Gary R. Weisman, Associate Professor of Chemistry



John J. Wright, Professor of Physics

29 April 1988
Date

CONTENTS

DEDICATION	v
ACKNOWLEDGEMENTS	vi
LIST OF ABBREVIATIONS	vii
LIST OF TABLES	viii
LIST OF FIGURES	xi
ABSTRACT	xii
CHAPTER	PAGE
INTRODUCTION	1
1 THEORETICAL BACKGROUND	4
1.1 Variational Principle and Molecular Orbital Theory	5
1.2 Hartree-Fock Theory	6
1.3 Multiconfiguration MO Method	9
1.3.1 Configuration Interaction (CI)	10
1.3.2 Multiconfiguration SCF (MCSCF) Method	11
1.4 Complete Active Space SCF (CASSCF) Method	13
1.5 Møller-Plesset Perturbation Theory	15
2 DETAILS OF THE COMPUTATIONS	17
2.1 The Molecular Systems	17
2.2 The Basis Sets	17
2.3 The Computational Procedure	20
3 RESULTS	24
3.1 Dilithioacetylene	24
3.1.1 Hartree-Fock Calculations	24
3.1.2 MCSCF-CASSCF Calculations	29

3.1.3	Møller-Plesset Calculations	36
3.2	Dilithiomethane	42
3.2.1	Hartree-Fock Calculations	42
3.2.2	MCSCF-CASSCF Calculations	55
3.2.3	CISD Calculations	68
4	DISCUSSION	69
4.1	Dilithioacetylene	69
4.1.1	Hartree-Fock Structures	69
4.1.2	MCSCF Structures	71
4.2	Dilithiomethane	83
4.2.1	Hartree-Fock Structures	83
4.2.2	MCSCF Structures	85
5	CONCLUSIONS	90
5.1	Dilithioacetylene	90
5.2	Dilithiomethane	92
	APPENDIXES	95
	LIST OF REFERENCES	104

DEDICATION

**TO MY PARENTS, WIFE AND SON
WHO HAVE WAITED SO PATIENTLY,
FOR SO LONG
ON THE OTHER SIDE OF THE EARTH**

ACKNOWLEDGEMENTS

I wish to express my lasting and sincere gratitude to my dissertation director, Professor Frank L. Pilar. For his giving of much time and energy in the course of this study, and for his friendship and guidance, I now tender my heartfelt thanks.

I am indebted to Professor Johnson for pointing out this topic to me, and to Professor Howard Mayne for his close reading and helpfull criticism of this thesis. I gratefully acknowledge Dr. Mike W. Schmidt at the North Dakota State University for his answering my many questions in using the GAMESS program.

I would also like to express my appreciation to the computer service staff at UNH, especially to Gerry Pregent and Elizabeth Rivet for their assistance in arranging the allocation of the computer time and storage space. My thanks are also due to the Cornell National Supercomputer Facility for computer time allocation.

I would not forget my brother, Shu-Chun; he certainly deserves my appreciation.

LIST OF ABBREVIATIONS

BSSE	Basis Set Superposition Effect
CASSCF	Complete Active Space Self-Consistent Field
CI	Configuration Interaction
CID	Configuration Interaction, Double
CISD	Configuration Interaction, Single and Double
CSF	Configuration State Function
GTO	Gaussian-type Orbital
HF	Hartree-Fock
LCAO	Linear Combination of Atomic Orbitals
MCSCF	Multiconfiguration Self-Consistent Field
MO	Molecular Orbital
MP	Møller-Plesset
MP2	Møller-Plesset second-order correction
MP3	Møller-Plesset third-order correction
MP4	Møller-Plesset fourth-order correction
RHF	Restricted Hartree-Fock
ROHF	Restricted Open-shell Hartree-Fock
SCF	Self-Consistent Field
STO	Slater-Type Orbital
UHF	Unrestricted Hartree-Fock

LIST OF TABLES

Table 1	RHF/STO-6G Optimized Geometries For C_2Li_2	25
Table 2	RHF Optimized Energies For C_2Li_2	27
Table 3	RHF Optimized Geometries For C_2Li_3	27
Table 4.1	RHF Mulliken Analyses For Linear C_2Li_2	28
Table 4.2	RHF Mulliken Analyses For Bridged C_2Li_2	28
Table 5.1	MCSCF Optimized Energies For Linear C_2Li_2	30
Table 5.2	MCSCF Optimized Energies For Bridged C_2Li_2	30
Table 6	MCSCF Relative Energies For C_2Li_2	31
Table 7	MCSCF Optimized Geometries For C_2Li_2	32
Table 8	The First Three Most Important CSFs in the MCSCF/STO-6G Wavefunction For C_2Li_2	34
Table 9	The First Three Most Important CSFs in the MCSCF/6-31G Wavefunction For C_2Li_2	35
Table 10	The First Three Most Important CSFs in the MCSCF/6-31G* Wavefunction For C_2Li_2	35
Table 11	MCSCF/STO-6G Mulliken Net Charges and Dipole Moments For C_2Li_2	37
Table 12	MCSCF/6-31G Mulliken Net Charges and Dipole Moments For C_2Li_2	38
Table 13	MCSCF/6-31G* Mulliken Net Charges and Dipole Moments For C_2Li_2	38
Table 14	Møller-Plesset Energies For Linear C_2Li_2	39
Table 15	Møller-Plesset Energies For Bridged C_2Li_2	40
Table 16	Møller-Plesset Relative Energies For C_2Li_2	41
Table 17	Singlet and Triplet HF Energies For CH_2Li_2	43
Table 18	Singlet and Triplet HF Relative Energies For CH_2Li_2	44
Table 19	Singlet and Triplet HF relative Energies For CH_2Li_2	45
Table 20.1	HF Optimized Geometries For CH_2Li_2 (tetra C_{2v})	47

Table 20.2	HF Optimized Geometries For CH ₂ Li ₂ (tetra C _{2v})	48
Table 21.1	HF Optimized Geometries For CH ₂ Li ₂ (cis C _{2v})	49
Table 21.2	HF Optimized Geometries For CH ₂ Li ₂ (cis C _{2v})	50
Table 22	HF Optimized Geometries For CH ₂ Li ₂ (trans D _{2h})	51
Table 23	Mulliken Net Charges and Dipole Moments For CH ₂ Li ₂ (tetra C _{2v})	52
Table 24	Mulliken Net Charges and Dipole Moments For CH ₂ Li ₂ (cis C _{2v})	53
Table 25	Mulliken Net Charges and Dipole Moments For CH ₂ Li ₂ (trans D _{2h})	54
Table 26	Mulliken Overlap Analyses For CH ₂ Li ₂ (tetra C _{2v})	56
Table 27	Mulliken Overlap Analyses For CH ₂ Li ₂ (cis C _{2v})	57
Table 28	Mulliken Overlap Analyses For CH ₂ Li ₂ (trans D _{2h})	58
Table 29	Singlet and Triplet MCSCF Energies For CH ₂ Li ₂	60
Table 30	MCSCF Relative Energies For CH ₂ Li ₂	61
Table 31	MCSCF Optimized Geometries For CH ₂ Li ₂ (Part 1)	62
Table 32	MCSCF Optimized Geometries For CH ₂ Li ₂ (Part 2)	63
Table 33	Mulliken MCSCF Overlap Analyses For CH ₂ Li ₂	64
Table 34	Mulliken MCSCF Net Charges For CH ₂ Li ₂	65
Table 35	The First Three Most Important CSFs in MCSCF Wavefunction For tetra CH ₂ Li ₂	66
Table 36	The First Three Most Important CSFs in MCSCF Wavefunction For cis CH ₂ Li ₂	66
Table 37	The First Three Most Important CSFs in MCSCF Wavefunction For trans CH ₂ Li ₂	67
Table 38	The <i>d</i> Function Superposition Effect For C ₂ Li ₂	72
Table 39.1	Occupation Numbers For the Active Space in C ₂ Li ₂ (n _a = 7, 196 CSFs)	74
Table 39.2	Occupation Numbers For the Active Space in C ₂ Li ₂ (n _a = 8, 1176 CSFs)	75
Table 39.3	Occupation Numbers For the Active Space in C ₂ Li ₂ (n _a = 9, 5292 CSFs)	76

Table 39.4	Occupation Numbers For the Active Space in C_2Li_2 ($n_a = 10$, 19404 CSFs)	77
Table 40	“Virtual” Occupation Numbers in the MCSCF/6-31G* Wavefunction For C_2Li_2	79
Table 41	Weights of the First Three Most Important CSFs in MCSCF Wavefunctions For C_2Li_2	80
Table 42.1	Occupation Numbers For the Active Space in CH_2Li_2 Part 1 (Singlet $n_a = 8$, 1764 CSFs)	86
Table 42.2	Occupation Numbers For the Active Space in CH_2Li_2 Part 2 (Triplet $n_a = 8$, 7560 CSFs)	87
Table 43	Weights of the First Three Most Important CSFs in MCSCF Wavefunctions For CH_2Li_2	89

LIST OF FIGURES

Figure 1	The Starting Geometries For C_2Li_2 and CH_2Li_2	18
Figure 2	Dependence of Energies of C_2Li_2 on Angle θ	82
Figure 3	Optimized Geometries For CH_2Li_2	84

ABSTRACT

AB INITIO MOLECULAR ORBITAL INVESTIGATIONS OF MOLECULAR STRUCTURES FOR LITHIATED HYDROCARBONS

By

Shu-Jun Su

University of New Hampshire, May 1988

Organolithium compounds are important reagents of widespread use in synthetic organic chemistry. Structures of organolithium hydrocarbons do not follow classical rules; replacement of a hydrogen by lithium in their molecules almost always results in a major change in geometry, electronic state, or both. The structures of many of these compounds still remain unknown and a subject of controversy.

This study investigated the geometries and electronic states of the ground states of dilithioacetylene and dilithiomethane molecules by using *ab initio* molecular orbital calculations. The geometries of both the molecules have been fully optimized at both the single determinant Hartree-Fock self consistent field (HF SCF) and the multiconfiguration self consistent field (MC SCF) levels with a variety of basis sets. Linear and planar bridged forms for dilithioacetylene and tetrahedral-like, cis planar, and trans planar forms for dilithiomethane were studied. The electronic states examined were the singlet state for both

molecules and the triplet state for dilithiomethane.

It has been found that the equilibrium geometries, a linear and a planar bridged structures for dilithioacetylene molecule, and a cis planar and a tetrahedral-like forms for the singlet and triplet states of dilithiomethane molecule, are rather sensitive to the choice of the basis set at the Hartree-Fock level of theory. Calculations at the MCSCF level of theory behave the same way but in smaller active multi configuration spaces, and do not seem to depend on the basis set in larger active spaces. Both the molecules have a relatively flat potential energy surface and do not exhibit strong preferences for the optimized structures. This lack of preference for the optimized structures is especially true for the MCSCF calculations on the multiplicity of the ground state structures for dilithiomethane molecule.

Introduction

Organolithium compounds are widely employed as synthetic intermediates in preparative organic chemistry[1]. Despite their obvious importance, relatively little is known experimentally regarding their structures[2]. Among other things, the strong tendency of lithium compounds to aggregate in the solid, in solution, and in the gas phase contributes to the complications of studying the structures and energies of the isolated monomers experimentally. In view of these difficulties, theoretical calculations afford the best source of such information. Since the geometries of small and moderately large molecules can be routinely calculated with considerable confidence [3-5], it appears that high level *ab initio* calculations should be capable of establishing the correct equilibrium structures of various kinds of lithiated hydrocarbon species. At the present time, there are about forty lithiohydrocarbons, in the sense that the lithium is associated with one or more carbon atoms, which have been studied at different levels of quantum chemical theory [6-32]. These nonempirical calculations have confirmed that lithium is capable of replacing many or all of the hydrogen atoms for a wide range of hydrocarbon species to form lithiated hydrocarbons, $C_nH_nLi_x$ with more than one lithium, and lithiocarbons, C_nLi_x . Two remarkable findings were made from these studies:

1. Some of these lithiated hydrocarbons may exist in unusual struc-

tures that would not be anticipated on the basis of conventional structure rules, i.e., the theory of tetrahedral carbon, or the van't Hoff-Le Bel hypothesis[34].

2. Some of these lithium compounds are unusual in having triplet ground states.

A number of such unusual structures are illustrated, e.g., those with propensities for anti-van't Hoff geometries (molecules with planar tetracoordinate carbon [6,7], etc.), those with ability to bridge two or more atoms in vicinal arrangements [14,17,19,20], those with multiple bridging involving two or more lithiums [19,20], and those participating in hypermetallated octet rule-violating stoichiometries [29,30]. The original literature provides details.

The exact geometric structures of some lithiated hydrocarbon species have long been a subject of some controversy. Particularly, the structure of the isolated dilithioacetylene molecule, C_2Li_2 , and the ground state configuration of the dilithiomethane molecule, CH_2Li_2 , still remain uncertain. In the case of the geometric conformation of dilithioacetylene, the theoretical results obtained by various authors are quite different [6]. In general, the energetically preferred geometry is basis set dependent. At the Hartree-Fock SCF level, Apeloig et al. [10] predicted the planar D_{2h} structure to be the lowest in energy, while Ritchie [31] found the slightly bent form, C_{2v} symmetry, to be the "true" minimum. Recently, Jaworski et al. [33] investigated the C_2Li_2 molecule up to the Coupled Cluster Configuration Interac-

tion level with the 6-311G* basis and concluded that the planar D_{2h} structure is predicted to be the minimum in energy. In the case of dilithiomethane, Collins et al. [6] claimed that it is difficult to assign the ground state configuration since the several examined geometries differ relatively little in energy.

The work reported in this dissertation was focused on the geometries and energies for both dilithioacetylene and dilithiomethane isomers. The theoretical calculations were carried out at the post Hartree-Fock as well as the Hartree-Fock *ab initio* SCF levels. More specifically, the investigation was done first at the Hartree-Fock single determinant SCF level of theory, then followed by the multiconfiguration SCF *ab initio* calculations using basis sets of different sophistication. In addition, Møller-Plesset (MP) perturbation and configuration interaction (CI) calculations were also performed on the dilithioacetylene and dilithiomethane molecules, respectively.

Chapter 1

Theoretical Background

All theoretical calculations carried out in this study are based on the molecular orbital theory (MO) and can be further classified into two main categories. One is the Hartree-Fock self-consistent field (SCF) level of theory, which is based on the single determinant description of the total wavefunction. Within the framework of the Hartree-Fock (HF) theory, the restricted Hartree-Fock (RHF), the unrestricted Hartree-Fock (UHF) and the restricted open-shell Hartree-Fock (ROHF) [35–42] methods are used in this research. The second category is based on the multideterminant superposition representation of the total wavefunctions. The multiconfiguration self-consistent field (MCSCF) method [43–48] and configuration interaction (CI) [49–52] fall into this category and are also employed in this work. Among several approaches of the MCSCF method, the complete active space self-consistent field (CASSCF) procedure [53–55] is used throughout the entire study reported in this dissertation. For the purpose of coherency and understanding, the theoretical methods used in this work are outlined briefly in this section.

1.1 Variational Principle and Molecular Orbital Theory

Under the Born-Oppenheimer approximation [56], the energy and many other properties of a stationary state of an n electron molecule can be obtained by solution of the Schrödinger partial differential equation

$$\hat{H} \Psi = E \Psi \quad (1.1)$$

where the nonrelativistic Hamiltonian \hat{H} in atomic units is

$$\hat{H} = - \sum_i \frac{1}{2} \nabla_i^2 - \sum_i \sum_a \frac{Z_a}{r_{ia}} + \sum_{i < j} \frac{1}{r_{ij}} + \sum_{a < b} \frac{Z_a Z_b}{R_{ab}} \quad (1.2)$$

The first term is the electronic kinetic energy operator for the i th electron, the second term is the potential energy operator between the i th electron and the a th nucleus (with charge Z_a), the third term is the electron-electron repulsion energy between the i th and j th electrons, and finally, the last term is the nucleus-nucleus repulsion energy with R_{ab} the distance between the a th and b th nucleus of respective charges Z_a and Z_b .

Given a normalized wavefunction Ψ that satisfies the appropriate boundary conditions

$$\langle \Psi | \Psi \rangle = 1 \quad (1.3)$$

the variational principle proves that the expectation value of the Hamiltonian value is an upper bound to the exact energy of the quan-

tum mechanical system in question

$$\langle \Psi | \hat{H} | \Psi \rangle \geq E_0 \quad (1.4)$$

Therefore the “best” wavefunction of a given form is the one that yields the lowest energy. To find out the “best” wavefunction the molecular orbital (MO) approximation has provided a theoretical framework for such a purpose. The rigorous mathematical treatment of the molecular orbital model is the Hartree-Fock approximation.

1.2 Hartree-Fock Theory

For closed-shell atoms and molecules the Hartree-Fock theory approximates the wavefunction Ψ in Eq.(1.4) as a Slater determinant [57]

$$\Psi = \mathcal{A}\psi = \mathcal{A}\phi_1\phi_2\dots\phi_n \quad (1.5)$$

in which \mathcal{A} is an antisymmetrizing operator for n electrons which guarantees that any interchange of the full space and spin coordinates of two electrons brings about a sign change in the wavefunction. The $\{\phi_i\}$ are spin orbitals, each of which is a one-electron function: a product of a spatial function and a one-electron spin function [α (spin up) or β (spin down)].

By minimizing the energy resulting from the single determinant wavefunction in Eq.(1.5) with respect to the choice of spin orbitals,

one can derive an equation, actually a set of integrodifferential equations, called the Hartree-Fock equations, which determine the optimal spin orbitals. Therefore the Hartree-Fock wavefunction is the best (in the variational sense) wavefunction which can be constructed by assigning each electron to a separate orbital, or function, depending only on the coordinates of that electron.

The solution to the Hartree-Fock equation is conducted in such a way that $\langle \Psi | \hat{H} | \Psi \rangle$ is minimized while the orbitals $\{\phi_i\}$ are generated until self consistency is reached.

Only for one-electron systems such as the hydrogen atom can the Hartree-Fock equations be solved in closed form. However, for many-electron atoms the Hartree-Fock equation may be solved to a rather high accuracy by numerical integration. For molecules one invariably expands the orbitals $\{\phi_i\}$ in terms of a set of analytic basis functions

$$\phi_i = \sum_{\mu}^m \chi_{\mu} c_{\mu i} \quad m \geq n \quad (1.6)$$

where $c_{\mu i}$ are the molecular orbital coefficients, and the set of atomic orbitals χ_{μ} is called a basis set. If the set of $\{\chi_{\mu}\}$ were complete, this would be an exact expression. Unfortunately, it is never possible to use a mathematically complete set of basis functions in molecular calculations of practical nature; thus one truncates the expression to m finite number of the basis functions. As such one can obtain approximate solutions to the Hartree-Fock wavefunction. If the $\{\chi_{\mu}\}$ are chosen as the atomic orbitals of the constituent atoms, this is known as the linear combination of atomic orbitals (LCAO) approximation. From Eq.(1.6), the problem of calculating the Hartree-Fock molecular orbitals reduces to the problem of calculating an optimal set of linear coefficients $c_{\mu i}$. That is, the coefficients are adjusted to minimize the

expectation value of the Hamiltonian

$$E = \langle \Psi | \hat{H} | \Psi \rangle / \langle \Psi | \Psi \rangle \quad (1.7)$$

where Ψ is any single determinant wavefunction. This implies the variational equations

$$\partial E / \partial c_\mu = 0 \quad \text{for all } \mu \quad (1.8)$$

The essential point is that the Hartree-Fock wavefunction is the best wavefunction, in the variational sense, which can be constructed by assigning each electron to a separate orbital depending only on the coordinates of that electron. The best (lowest energy) single-determinant wavefunction constructed within a finite basis set is the self-consistent field (SCF) wavefunction. Most of the electronic structure calculations reported in this work are of the SCF variety.

In practical calculation of Hartree-Fock wavefunctions one must be more specific about the spin orbitals $\{\phi_i\}$. There are two types of spin orbitals: restricted spin orbitals, which are constrained to have the same spatial function for α and β spin functions; and unrestricted spin orbitals, which have different spatial functions for each pair of α and β spin functions. The solution of the Hartree-Fock equations employing restricted spin orbitals yields the restricted Hartree-Fock (RHF) wavefunction. For a RHF wavefunction each of the occupied spatial molecular orbitals is doubly occupied.

Obviously, not all molecules, nor all states of closed-shell molecules, can be described by pairs of electrons in restricted orbitals. In deal-

ing with such open-shell problems, there are two approaches: the unrestricted open-shell (UHF) and the restricted open-shell (ROHF) procedures. In the UHF formalism, the spin orbitals for a closed-shell electron pair are no longer assumed to be equal, and all electrons occupy different spatial orbitals. In the ROHF formalism, all electrons, except those that are explicitly required to occupy open-shell orbitals, occupy closed-shell orbitals, that is, each pair of α and β electrons shares the same spatial function.

1.3 Multideterminant MO Methods

In the Hartree-Fock approximation, the electrons interact among themselves only in the presence of an average potential field. The Pauli principle keeps electrons with parallel spin (in different orbitals) away from each other, but it has nothing to offer to electrons with antiparallel spin in the same molecular orbital. That is the major deficiency of the Hartree-Fock method which prevents the obtaining of reliable results in some aspects of chemical interest. Accounting for details of electronic motions beyond the Hartree-Fock level is usually referred to as the *electron correlation* problem. Many schemes have been devised and employed for that purpose, such as unrestricted and extended Hartree-Fock methods, multiconfiguration SCF, perturbation

theory, and configuration interaction.

1.3.1 Configuration Interaction (CI)

Configuration interaction [58], abbreviated CI, starts with a single determinant calculation as usual. The molecular orbitals thus obtained are used to construct excited states of the appropriate symmetry by promoting electrons from ground state orbitals to all virtual orbitals. The linear variational method is then applied to find the best possible mixing coefficients

$$\Psi = \sum_i C_i \Phi_i \quad (1.9)$$

where the Φ_i represent particular assignments of electrons to orbitals and are called configuration state functions (CSFs). Particularly, the first term in Eq.(7), Φ_0 , is the SCF wavefunction. All of the other Φ_i are formed by replacing one, two, ... or all the occupied spin MO's with the virtual MO's. If the summation \sum_i is over all possible substituted determinants, it leads to the full configuration interaction method. The difference between the Hartree-Fock energy with a given basis set and the full CI energy with the same basis set is the *correlation energy* within the basis.

Since the total number of the CSFs constructed for an n electron system in a basis set of N functions is given by

$$(2N)!/[n!(2N - n)!]$$

as the basis set becomes more complete, that is, as the number of basis functions $N \rightarrow \infty$, the full CI method is not practical. Many

procedures therefore have been designed to limit the length of the CI expansion. The most straightforward way to do so is to truncate the series at a given level of electron substitution. Among them, two types of truncated CI are most widely used. One is the double substituted CI, termed *Configuration Interaction, Doubles* or CID

$$\Psi_{CID} = C_0\Phi_0 + \sum \sum_{i<j}^{occ} \sum \sum_{a<b}^{virt} C_{ij}^{ab} \Phi_{ij}^{ab} \quad (1.10)$$

in which all Φ_{ij} are constructed by replacing two, and only two, occupied MO's with two virtual MO's at a time; and the other is the single and double substituted CI, termed *Configuration Interaction, Singles and Doubles* or CISD

$$\Psi_{CISD} = C_0\Phi_0 + \sum_i \sum_a^{occ} C_i^a \Phi_i^a + \sum \sum_{i<j}^{occ} \sum \sum_{a<b}^{virt} C_{ij}^{ab} \Phi_{ij}^{ab} \quad (1.11)$$

in which both the single and double substitutions are included.

1.3.2 Multiconfiguration SCF (MCSCF) Method

The mixing of electronic states can also be achieved by considering more than one configuration at the SCF level. That leads to the multiconfiguration self-consistent field (MCSCF) method [48]. The central idea is that the MCSCF wavefunction is a truncated CI expansion

$$\Psi_{MCSCF} = \sum_i C_i \Phi_i \quad (1.12)$$

where each of the CSF expansion terms Φ_i is a Slater determinant of orthonormal molecular orbitals ϕ_i .

The formal basis of the MCSCF methods lies in the following two assumptions:

1. The CSF terms, which depend on the orbitals, determine the Hamiltonian matrix elements;
2. The shape of the orbitals then affect the eigenvalues of the Hamiltonian matrix expanded in terms of a limited CSF basis.

For a fixed CSF expansion, the shape of the orbitals may be varied, thereby producing different approximate energies. A particular choice of orbital set that gives the lowest approximate energy, and therefore the closest approximation to the exact energy, gives the best wavefunction for the given CSF expansion. However, the energy minimization with respect to orbitals alone does not guarantee a good agreement of the approximate energy with the exact energy. This agreement is achieved with a combination of the appropriate choice of CSF expansion set and of orbital optimization for this chosen expansion set. Therefore, minimizing $\langle \Psi_{MCSCF} | \hat{H} | \Psi_{MCSCF} \rangle$, with respect to orbital variations and CSF expansion coefficient variations would lead to an MCSCF wavefunction which is the best approximate wavefunction to the exact wavefunction for the given choice of CSF's. In other words, for a MCSCF wavefunction in Eq. (1.12), both the expansion coefficients C_i and the orthonormal orbitals contained in Φ_i are optimized simultaneously. In other words, in an MCSCF procedure, an effective one-particle potential is adjusted until self-consistency is obtained for all of the electrons of a molecular system and that is

done for a wavefunction that consists of the superposition of several electronic configurations, i.e., CSFs.

1.4 The CASSCF Method

The complete active space self-consistent field (CASSCF) method [53–55] is a special approach to the MCSCF method. It originally was developed from a scheme to select CSFs and turns out to be an outstanding development for optimizing the variables in an MCSCF wavefunction.

A CASSCF study normally starts by defining an orthonormal molecular orbital space

$$\phi_i(\mathbf{r}) \quad i = 1, 2, \dots, m \quad (1.13)$$

Normally these molecular orbitals are obtained as expansions in a set of atom-centered basis functions, m being the number of such functions and, in principle, infinite. Then an CASSCF calculation begins by dividing the molecular orbital space into three subspaces: the inactive, the active and the external orbitals. The inactive and active subspaces constitute the internal (occupied) orbital subspace, while the external orbitals constitute the unoccupied subspace. It should be noted that some of the virtual orbitals in a RHF wavefunction are included in the active subspace. The configuration state functions Φ_i are then generated from these orbitals in the following way:

- The inactive orbitals are doubly occupied in all CSFs, these orbitals then have occupation numbers exactly equal to 2;
- The remaining (active) electrons occupy the active orbitals; the active orbitals have occupation numbers varying between 0 and 2. Using these electrons and orbitals, a full list of CSFs which have the required spin and spatial symmetry is constructed.

The inactive orbitals represent an “SCF sea” in which the active electrons move around. By the graphic unitary group approach (GUGA) [59], all necessary information about the CSFs and their relative ordering is contained in a compressed table called the distinct row table (DRT) [59]. The CASSCF wavefunction is formed as a linear combination of all these CSFs, constituting a complete expansion in the active orbital subspace. That is, once the inactive and active orbitals are chosen, the wavefunction is completely specified. The optimization step then consists of finding those expansion coefficients in Eq.(1.12) and the molecular orbitals that make the energy stationary with respect to all parameters.

A number of procedures for performing the optimization can be found in the literature [60]. In this study, the non-linear Newton-Raphson procedure [60-63] was used. It actually solves a linear equation system

$$\begin{pmatrix} \mathbf{g}^{(c)} \\ \mathbf{g}^{(o)} \end{pmatrix} + \begin{pmatrix} \mathbf{H}^{(cc)} & \mathbf{H}^{(co)} \\ (\mathbf{H}^{(co)\dagger})^\dagger & \mathbf{H}^{(oo)} \end{pmatrix} \begin{pmatrix} \mathbf{S} \\ \mathbf{T} \end{pmatrix} = 0 \quad (1.14)$$

where $\mathbf{g}^{(c)}$ and $\mathbf{g}^{(o)}$ are the gradients (c for the configuration and o for the orbital part), \mathbf{H} is Hessian matrix, and \mathbf{S} and \mathbf{T} are parameters

that constitute a set of variables that can be used to determine the stationary point of the energy. Equation (1.12) is solved iteratively for \mathbf{S} and \mathbf{T} until the convergence criteria are fulfilled to the desired accuracy.

The strength of the CASSCF method lies in its simplicity. It is a pure orbital method in the sense that one only has to worry about selecting an appropriate inactive and active orbital space in order to define the CAS wavefunction.

1.5 Møller–Plesset Perturbation Theory

The perturbation theory of Møller–Plesset [64] is an alternative approach to the *correlation* problem. This model partitions the Hamiltonian as

$$\hat{H}_\lambda = \hat{H}_0 + \lambda\hat{V} \quad (1.15)$$

where \hat{H}_0 (the zeroth-order Hamiltonian) is the Hartree-Fock operator

$$\hat{H}_0 = \sum_i f(i) = \sum_i (h(i) + v^{HF}(i)) \quad (1.16)$$

and

$$\lambda\hat{V} = \lambda(\hat{H} - \hat{H}_0) \quad (1.17)$$

is called the perturbation. Here \hat{H} is the correct Hamiltonian and λ is a dimensionless parameter. Clearly \hat{H}_λ coincides with \hat{H}_0 if $\lambda = 0$, and with \hat{H} if $\lambda = 1$. Ψ_λ and E_λ , the exact (within a given basis)

ground state wavefunction and energy for a system described by the Hamiltonian \hat{H}_λ , may now be expanded in power of λ

$$\Psi_\lambda = \Psi^0 + \lambda \Psi^{(1)} + \lambda^2 \Psi^{(2)} + \dots \quad (1.18)$$

$$E_\lambda = E^0 + \lambda E^{(1)} + \lambda^2 E^{(2)} + \dots \quad (1.19)$$

Practical correlation methods may now be formulated by setting the parameter $\lambda = 1$ and by truncation of the series in Eq.(1.18–1.19) to various order. Therefore truncation after second order results in MP2 method, after third order in MP3 and so forth.

Chapter 2

Details of The Computations

2.1 The Molecular Systems

Two groups of lithiated hydrocarbon isomers, six each for dilithioacetylene C_2Li_2 and dilithiomethane CH_2Li_2 , were computationally studied in this work. Figure 1 shows their structures and spatial symmetries. **1 – 6** are the isomers for C_2Li_2 in the singlet state, **7 – 9** are the starting geometries for CH_2Li_2 in the singlet and triplet state.

2.2 The Basis Sets

Three types of basis sets: minimal, split-valence and polarization, were used throughout the entire work reported in this dissertation.

The minimal basis set used was STO-6G [65–66]. This basis set representation for hydrogen, lithium and carbon comprises the following atomic functions

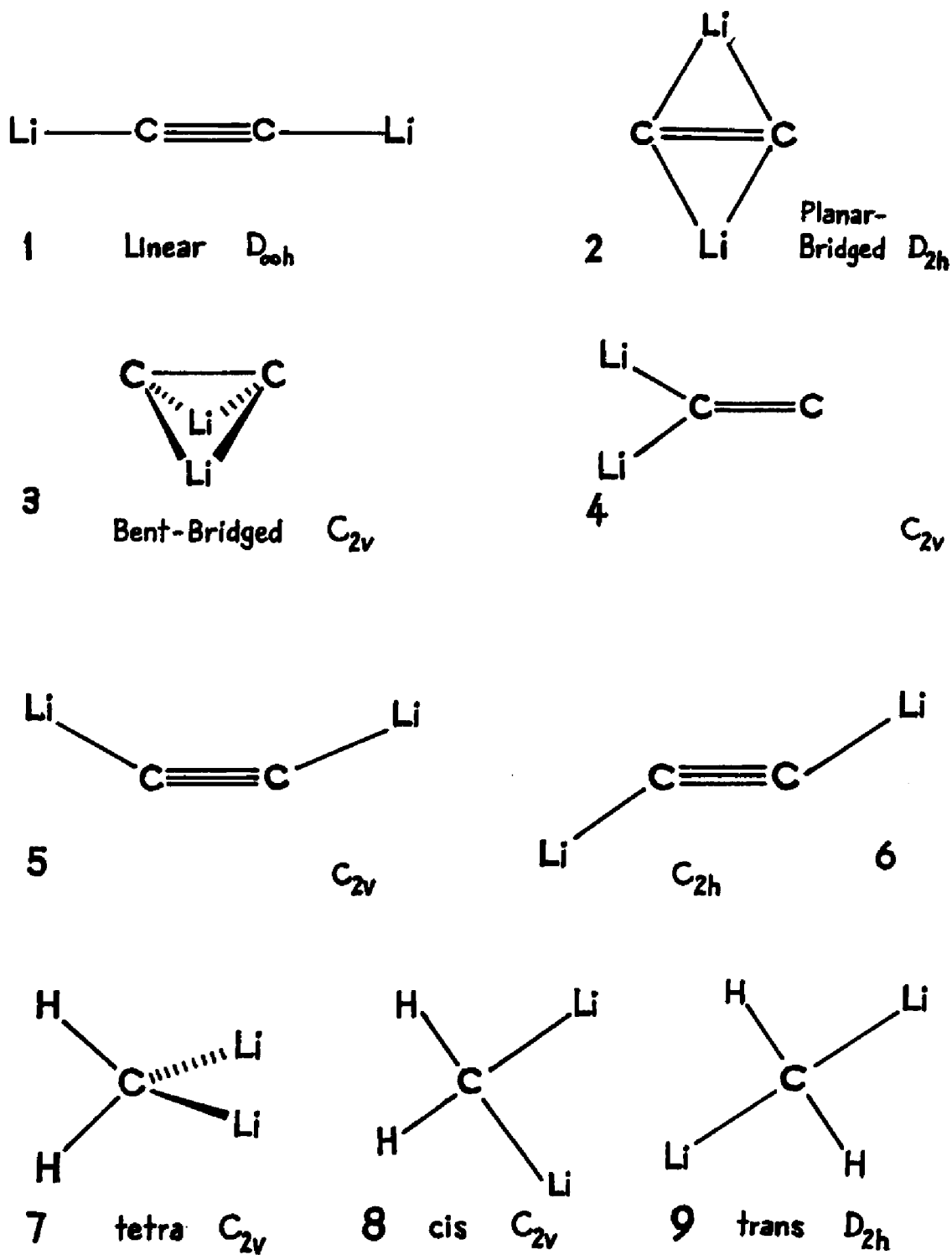


Figure 1. The Starting Geometries For C_2Li_2 and CH_2Li_2

H: 1s

Li and C: 1s, 2s, 2p_x, 2p_y, 2p_z

Each atomic function is expanded in terms of six gaussian functions.

In a split-valence basis set [67-69], hydrogen is represented by two s-type functions, and lithium and carbon by two complete sets of valence s and p functions.

H: 1s', 1s''

Li and C: 1s', 2s', 2p_x', 2p_y', 2p_z', 2s'', 2p_x'', 2p_y'', 2p_z''

Here the basis functions comprising the two valence shells are denoted ' and '', respectively. Each basis function is then represented by a linear combination of gaussian functions.

The 6-31G split-valence basis set was actually used in this work. It comprises inner-shell functions each expressed in terms of a linear combination of six gaussians, and the two split valence-shells represented by three and one gaussians, respectively.

Li and C: 1s' — 6 gaussians

2s' — 3 gaussians

2s'' — 1 gaussian

2p_x', 2p_y', 2p_z' — 3 gaussians each

2p_x'', 2p_y'', 2p_z' — 1 gaussian each

H : 1s' — 3 gaussians

1s" — 1 gaussians

The polarization basis sets used in this work were 6-31G* and 6-31G** [70–72]. The 6-31G* basis set is constructed by the addition of a set of six *d*-type gaussian functions to the split-valence 6-31G basis set representation for each heavy (non-hydrogen) atom. The *d*-type functions are a single set of 3*d* primitive gaussians¹. For computational convenience, there are “six” 3*d* functions per atom — $3d_{xx}$, $3d_{yy}$, $3d_{zz}$, $3d_{xy}$, $3d_{yz}$, and $3d_{zx}$. These six, the Cartesian gaussians, are linear combinations of the usual five 3*d* functions — $3d_{xy}$, $3d_{x^2-y^2}$, $3d_{yz}$, $3d_{zx}$, and $3d_{z^2}$ and a 3*s* function. The 6-31G** basis set is identical to 6-31G* except for the addition of a set of three p-type gaussian functions to hydrogen atoms. It is obvious that the 6-31G* and 6-31G** basis sets are the same for the C₂Li₂ system since no hydrogen atoms are present.

In addition, the Dunning-Hay (9s 5p)/[3s 2p], abbreviated D95V, contracted basis set [73] and the 6-311G split valence basis set and the 6-311G* basis were used in parts of this work. The Dunning-Hay basis set is a contracted one and uses disjoint subsets of primitives so that no primitive appears in more than one basis function. In this work, the Dunning-Hay D95V basis set used is

H: (4s)/[2s]

C and Li: (9s 5p)/[3s 2p]

¹Primitive gaussians are individual gaussian functions used to construct basis functions

These descriptions stand for a contraction scheme. For H, it is represented by two *s*-atomic orbitals, each of which is a linear combination of 4 gaussian primitives; for Li and C, the nine primitives of *s*-type symmetry are contracted to three basis functions and the five primitives of *p*-type symmetry are contracted to two basis functions. This particular size, (9*s* 5*p*), is chosen based on its performance in the sense of both the accuracy and the computing time. It is well known that for a basis set of size *m*, the number of two-electron integrals which must be computed increases rapidly with the number of functions (as m^4). This (9*s* 5*p*)/[3*s* 2*p*] contraction reduces the number of basis functions from 24 to 9, therefore it can save a great deal of CPU time almost without any loss of accuracy.

2.3 The Computational Procedure

Ab initio Hartree-Fock and MCSCF-CASSCF calculations with and without geometry optimization were carried out. All MCSCF calculations were performed with the GAMESS program [5]. All Hartree-Fock single point calculations were done mostly with GAMESS as well as GAUSSIAN 82 [4] and GAUSSIAN 86 [74].

For both groups of C₂Li₂ ,and CH₂Li₂ ,the first step of the calculations was to perform RHF (UHF for the triplet states of CH₂Li₂) geometry optimization with STO-6G basis on the standard structures [65, 75-

76]. For the C_2Li_2 group, there are six starting structures with four types of symmetries; for the CH_2Li_2 group, there are three starting structures with two types of symmetries (see Figure 1).

As the next step, for the C_2Li_2 group, since the six starting structures were optimized to two symmetries in the first step of calculations (one is a linear form and the other is a planar bridged form), *ab initio* geometry optimizations were carried out only on the linear and planar-bridged forms in the sequence of ascertaining the theoretical level; that is, first the Hartree-Fock single determinant optimization was performed and this was followed by the multiconfiguration SCF geometry optimization; at each level of theory, geometry optimization was preceded by using more and more sophisticated basis sets. Within the MCSCF method, the inactive subspace was chosen as all of the core orbitals only, which is four orbitals, then CASSCF calculations were conducted in the order of increasing active subspaces from seven, eight, nine, and up to ten active orbitals. That is, with ten valence electrons activated for C_2Li_2 , the active space was changed as follows:

- At first it consisted of seven active orbitals and the wavefunction comprised 196 configurations.
- Then it was changed to eight active orbitals and yielded a wavefunction of 1176 configurations.
- Next it was increased to nine active orbitals and resulted in a 5292 configuration wavefunction.

- Finally, the active space was constituted from ten orbitals and led to a wavefunction made with 19404 configurations.

For the group of CH_2Li_2 isomers, the second step was the same as that for the C_2Li_2 group within the Hartree-Fock level, but a slightly different procedure was used at the MCSCF level. The inactive subspace was also chosen as all core orbitals which is three, but the size of the active subspace did not change at all. The MCSCF calculations were performed only on one fixed size of active subspace, that is, an eight orbital active space for the singlet state and a nine orbital active space for the triplet state. With all eight valence electrons participating, the wavefunction contained 1760 CSF's for the singlet state and 7650 CSF's for the triplet state.

In addition, for the singlet state for the dilithiomethane molecule, geometry optimizations of configuration interaction with all single and double substitution from the Hartree-Fock determinant, i.e., CISD, were also performed with 6-31G* basis set.

Finally, all geometry optimization calculations were carried out in such a way that each of them used the geometry obtained from the previous optimization at a lower level or with a simpler basis set as its input. In other words, a geometry optimized at lower theoretical level or with a simpler basis set was used as an starting point for the next optimization at a higher theoretical level or with a more complicated basis set.

Chapter 3

Results

Results from this theoretical research are reported in two parts: one for the dilithioacetylene C_2Li_2 structures and the other for the dilithiomethane CH_2Li_2 structures.

3.1 Dilithioacetylene

3.1.1 Hartree-Fock Calculations

Geometry optimization at the RHF/STO-6G level was initially carried out on the six starting structures with the four different symmetries shown in Figure 1. The RHF/STO-6G optimized structures and energies are presented in Table 1. This shows clearly that the six starting structures which belonged to four different symmetry groups were optimized to two symmetries, that is, a linear form with $D_{\infty h}$ symmetry, **1**, and a planar-bridged form with D_{2h} symmetry, **2**. The structures **3**, **4** and **6** were together optimized to the symmetry of

Table 1. RHF/STO-6G Optimized Geometries[†] For C₂Li₂

Starting Geometries				Optimized Structures			
Symmetry	R _{CC}	R _{CLi}	R _{LiLi}	Symmetry	R _{CC}	R _{CLi}	R _{LiLi}
D _{∞h}	1.200	1.800		D _{∞h}	1.220	1.810	
D _{2h}	1.200	1.900		D _{2h}	1.266	1.905	3.590
C _{2v}	1.260	1.250	1.654	D _{2h}	1.266	1.904	3.590
C _{2v}	1.200	1.800		D _{2h}	1.266	1.904	3.590
C _{2v}	1.200	1.800		D _{∞h}	1.200	1.810	
C _{2h}	1.200	1.800		D _{2h}	1.266	1.905	3.590

[†] Bond length in Å unit

the structure **2** which is D_{2h} while the structure **5** (trans bent) was stretched to a linear symmetry. At this level, the linear form of C_2Li_2 , **1**, was found to be less stable than the planar bridged one, **2**, by about 19 kcal/mol. All subsequent calculations were performed only on the linear and planar bridged forms of dilithioacetylene.

Geometry optimization with the split valence 6-31G, Dunning-Hay contracted (9s 5p)/[3s 2p], 6-311G and polarization 6-31G* basis sets were then carried out. Each optimization with a more complicated basis employed a structure optimized with a relatively simpler basis set as a starting geometry. The RHF optimized energies and structures with these basis sets are given in Tables 2 and 3, respectively. As can be seen from these, the Hartree-Fock relative energies of the linear C_2Li_2 vs. the planar bridged one are basis dependent. In general, if the polarization functions are not included in the basis set (using all but the minimal STO-6G basis), the linear $D_{\infty h}$ form is found to be more stable than the planar bridged D_{2h} . However, if d orbitals are added, the planar bridged was predicted to be lower in energy. However Ritchie [31] found the bent form (C_{2v} symmetry) to be the minimum. Though the bond lengths of C—C and C—Li are shorter in the linear C_2Li_2 than in the planar bridged form, the differences are very small and generally fall in a range of 0.01 to 0.02 Å. Comparing the Mulliken net charges [76] that are included in Table 4, one can see more accumulation of negative charges on the carbon atoms in the linear C_2Li_2 . The overlap population between carbon atoms

Table 2. RHF Optimized Energies For C_2Li_2

Basis	Linear $D_{\infty h}$		Planar Bridged D_{2h}	
	Energy (a.u.)	ΔE^\dagger	Energy (a.u.)	ΔE^\dagger
STO-6G	-90.284786	0.0	-90.316215	19.7
6-31G	-90.525607	-9.3	-90.510708	0.0
D95V [†]	-90.539673	-6.5	-90.529369	0.0
6-311G	-90.555594	-4.3	-90.548812	0.0
6-31G*	-90.550953	0.0	-90.561614	-6.7
6-311G*	-90.577568	0.0	-90.587950	-6.5

[†] $\Delta E = E_{Linear} - E_{Bridged}$ in kcal/mol

[‡]D95V is the Dunning-Hay (9s 5p)/[3s 2p] contracted basis

Table 3 RHF Optimized Geometries For C_2Li_2

	Linear $D_{\infty h}$		Planar Bridged D_{2h}		
	$R_{CC}(\text{\AA})$	$R_{CLi}(\text{\AA})$	$R_{CC}(\text{\AA})$	$R_{LiLi}(\text{\AA})$	$R_{CLi}(\text{\AA})$
STO-6G	1.220	1.811	1.270	3.592	1.904
6-31G	1.246	1.892	1.263	3.931	2.064
D95V	1.256	1.903	1.269	3.945	2.072
6-311G	1.241	1.876	1.255	3.865	2.068
6-31G*	1.235	1.900	1.250	3.856	2.068
6-31G**	1.23	1.90	1.25	3.86	

Table 4.1 RHF Mulliken Analyses For Linear C₂Li₂

Basis	Net Charge		Overlap Population	
	C	Li	C—C	C—Li
STO-6G	-0.10	0.10		
6-31G	-0.45	0.45		
D95V	-0.49	0.49	1.44	0.64
6-311G	-0.60	0.60	1.86	0.51
6-31G*	-0.32	0.32	2.05	0.73
6-311G*	-0.48	0.48	1.99	0.66

Table 4.2 RHF Mulliken Analyses For Planar-Bridged C₂Li₂

Basis	Net Charge		Overlap Population		
	C	Li	C—C	Li—Li	C—Li
STO-6G	-0.08	0.08			
6-31G	-0.40	0.40	0.69	0.12	0.35
D95V	-0.45	0.45	1.04	0.07	0.32
6-311G	-0.52	0.52	0.47	0.07	0.29
6-31G*	-0.22	0.22	1.16	0.08	0.49
6-311G*	-0.41	0.41	1.17	0.02	0.40

and between carbon atom and its adjacent lithium atom in the linear C_2Li_2 is much larger than that in the planar bridged one. Addition of d functions greatly increases the overlap between the carbon atoms in the planar bridged form.

3.1.2 MCSCF-CASSCF Results

All RHF/STO-6G, RHF/6-31G and RHF/6-31G* optimized structures were reoptimized with the same basis sets but at the multi-configuration self-consistent field, MCSCF, level. Tables 5, 6 and 7 summarize the MCSCF CASSCF energies, the relative energies (linear vs. planar-bridged) and optimized geometries, respectively. Due to the fact that the run of MCSCF/STO-6G optimization with 66 configurations (CSF) for the planar bridged C_2Li_2 never converged, no results for this are given.

With the minimal STO-6G basis, in smaller active spaces, (i.e., number of configurations (CSF) equal to 66, 196 and 1176), the planar bridged C_2Li_2 is lower in energy. The energy difference between the linear and bridged forms first increases with the increase in the number of configurations until the active space with 1176 configurations is reached; afterwards the linear structure becomes energy-favorable and continues to maintain this position relative to the planar bridged structure. With the split valence 6-31G basis, the situation is un-

Table 5.1 MCSCF Optimized Energies For Linear C₂Li₂

Number of Configurations	Energy (a.u.)		
	STO-6G	6-31G	6-31G*
66	-90.367617	-90.598088	-90.615960
196	-90.372332	-90.601748	-90.619279
1176	-90.392039	-90.618247	-90.650644
5292	-90.427832	-90.653415	-90.669064
19404	-90.432160	-90.664512	-

Table 5.2 MCSCF Optimized Energies for Bridged C₂Li₂

Number of Configurations	Energy (a.u.)		
	STO-6G	6-31G	6-31G*
66	-90.385739	-	-90.624062
196	-90.389202	-90.591434	-90.627029
1176	-90.412267	-90.613190	-90.647245
5292	-90.422174	-90.623972	-90.657453
19404	-90.425363	-90.66	-

Table 6. MCSCF Relative Energies For C_2Li_2

Number of Configurations	$\Delta E^\dagger_{Linear-Bridged}$		
	STO-6G	6-31G	6-31G ⁺
66	11.4	-	5.1
196	10.6	-6.5	4.9
1176	12.7	-3.2	-2.1
5292	-3.6	-18.5	-7.3
19404	-4.3	-	-

[†] in kcal/mol

Table 7. MCSCF Optimized Geometries For C_2Li_2

Basis	Number of Configurations	Linear $D_{\infty h}$		Planar Bridged D_{2h}		
		$R_{CC}(\text{\AA})$	$R_{CLi}(\text{\AA})$	$R_{CC}(\text{\AA})$	$R_{LiLi}(\text{\AA})$	$R_{CLi}(\text{\AA})$
STO-6G	66	1.246	1.815	1.284	3.566	1.895
	196	1.251	1.811	1.287	3.563	1.894
	1176	1.249	1.829	1.283	3.597	1.909
	5292	1.262	1.830	1.284	3.622	1.922
	19404	1.267	1.827	1.286	3.617	1.919
6-31G	66	1.265	1.892	-	-	-
	196	1.269	1.891	1.286	3.883	2.045
	1176	1.266	1.905	1.282	3.915	2.060
	5292	1.282	1.904	1.283	3.947	2.075
	19404	1.282	1.907			
6-31G*	66	1.255	1.896	1.270	3.821	2.013
	196	1.258	1.895	1.273	3.818	2.012
	1176	1.273	1.896	1.270	3.847	2.026
	5292	1.270	1.908	1.270	3.873	2.038

ambiguous: the linear C_2Li_2 is always more stable than the planar bridged in all sizes of the active subspaces that this research could consider. In the polarized 6-31G* basis set optimization, the changes in the MCSCF energy repeated the pattern found in the STO-6G calculations. That is, the linear form of $D_{\infty h}$ is still favored in energy over the planar D_{2h} form at larger active subspaces. But with the MCSCF/6-31G* geometry optimized in 5292-configuration space, the MCSCF/6-31G* calculation without geometry optimization (in 19404 configuration space) surprisingly showed that the energy difference between the linear and the planar bridged C_2Li_2 decreased to 0.65 kcal/mol only, with the linear form still lower in energy.

The results of the MCSCF structures optimized in different subspaces are presented in Table 7; one finds that the electron correlation lengthens the C—C bond in the linear C_2Li_2 by about 0.02 Å but makes no difference in the C—C bond of the bridged form. It is also seen from Table 7 that the inclusion of electron correlation stretches the C—Li distance in both forms of C_2Li_2 . However, the addition of *d* orbitals led to shortening of the C—C bond length compared to that occurring in STO-6G and 6-31G basis sets.

Tables 8 – 10 list the linear combination coefficients, the C_i in Eq.(7), of the first three most important configurations, in these wavefunctions. This shows that the contribution from the ground state configuration to the wavefunction, C_0 , is decreased with the increase in the size of the active subspace while the coefficients of the excited

Table 8. The First Three Most Important CSFs in
The MCSCF/STO-6G Wavefunction For C_2Li_2

Number of Configurations	Linear			Planar Bridged		
	First	Second	Third	First	Second	Third
66	0.97	0.14	0.12	0.97	0.12	0.12
196	0.96	0.15	0.13	0.97	0.12	0.11
1176	0.94	0.15	0.14	0.93	0.25	0.12
5292	0.93	0.18	0.13	0.92	0.26	0.12
19404	0.91	0.22	0.15	0.92	0.26	0.11

Table 9. The First Three Most Important CSFs in
the MCSCF/6-31G Wavefunction For C_2Li_2

Number of Configurations	Linear			Planar Bridged		
	First	Second	Third	First	Second	Third
66	0.97	0.13	0.11	-	-	-
196	0.96	0.14	0.12	0.97	0.13	0.12
1176	0.93	0.27	0.12	0.90	0.38	0.11
5292	0.92	0.24	0.11	0.88	0.36	0.11
19404	0.95	0.12	0.12			

Table 10. The First Three Most Important CSFs
in the MCSCF/6-31G* Wavefunction For C_2Li_2

Number of Configurations	Linear			Planar Bridged		
	First	Second	Third	First	Second	Third
66	0.97	0.12	0.11	0.97	0.12	0.11
196	0.97	0.13	0.12	0.97	0.12	0.12
1176	0.92	0.27	0.12	0.95	0.18	0.11
5292	0.93	0.22	0.11	0.93	0.23	0.11
19404 [†]	0.95	0.12	0.11	0.96	0.11	0.10

[†] using the optimized geometry in 5292 CSF space

state configurations, especially that of the second most important CSF, are increased with the expansion of the active space.

The Mulliken net charges are presented in Tables 11–13. As can be seen, electron correlation reduces Mulliken net charges on the carbon and lithium atoms in both the linear and bridged C_2Li_2 . Moreover, the change in Mulliken net charges in the bridged form of C_2Li_2 is larger than that in the linear form.

3.1.3 Møller-Plesset (MP) Calculations

The Møller-Plesset perturbation calculations of the second order correction (MP2), third order (MP3) and fourth order (MP4) with the STO-6G, 6-31G and 6-31G* basis sets on the MCSCF optimized geometries are shown in Tables 14 and 15. With 6-31G split valence basis, MP results (MP2, MP3, MP4SDQ, and MP4SDTQ) predict the linear form of C_2Li_2 to be more stable than the bridged one while both MP/STO-6G and MP/6-31G* results reach totally different conclusions, viz., the planar bridged one is the minimum in energy. Table 16 shows the MP relative energies of the linear vs. the bridged forms of C_2Li_2 .

Table 11. MCSCF/STO-6G Mulliken Net Charges and Dipole Moments
For C_2Li_2

Number of CSFs	Linear $D_{\infty h}$			Bridged D_{2h}		
	Net Charge		Dipole Moment	Net Charge		Dipole Moment
	C	Li	Debye	C	Li	Debye
66	-0.12	0.12	-	-0.11	0.11	-
196	-0.12	0.12	-	-0.11	0.11	-
1176	-0.11	0.11	-	-0.08	0.08	-
5292	-0.11	0.11	-	-0.08	0.08	-
19404	-0.09	0.09	-	-0.07	0.07	-

Table 12. MCSCF/6-31G Mulliken Net Charges and Dipole Moments
For C₂Li₂

Number of CSFs	Linear D _{∞h}			Bridged D _{2h}		
	Net Charge		Dipole Moment	Net Charge		Dipole Moment
	C	Li	Debye	C	Li	Debye
66	-0.47	0.47	-	-	-	-
196	-0.47	0.47	-	-0.43	0.43	-
1176	-0.43	0.43	-	-0.38	0.38	-
5292	-0.43	0.43	-	-0.38	0.38	-
19404	-0.42	0.42	-	-	-	-

Table 13. MCSCF/6-31G* Mulliken Net Charges and Dipole Moments
For C₂Li₂

Number of CSFs	Linear D _{∞h}			Bridged D _{2h}		
	Net Charge		Dipole Moment	Net Charge		Dipole Moment
	C	Li	Debye	C	Li	Debye
66	-0.35	0.35	-	-0.27	0.27	-
196	-0.35	0.35	-	-0.27	0.27	-
1176	-0.35	0.35	-	-0.23	0.23	-
5292	-0.32	0.32	-	-0.22	0.22	-

Table 14. Moller-Plesset Energies For Linear C₂Li₂

Model	Energy (a.u.)				
	MP2	MP3	MP4DQ	MP4SDQ	MP4SDTQ
1	-90.467245	-90.455779	-90.463619	-90.464600	-90.472238
2	-90.467867	-90.455904	-90.463869	-90.464847	-90.472622
3	-90.467780	-90.455948	-90.463972	-90.464966	-90.472720
4	-90.469213	-90.455987	-90.464429	-90.465424	-90.473578
5	-90.469579	-90.455878	-90.464446	-90.465438	-90.473726
6	-90.714941	-90.710303	-90.714243	-90.718961	-90.729998
7	-90.716196	-90.710305	-90.715327	-90.719086	-90.730236
8	-90.717460	-90.711608	-90.716632	-90.720400	-90.731566
9	-90.718728	-90.712153	-90.717422	-90.721318	-90.732829
10	-90.718793	-90.711977	-90.717326	-90.721263	-90.732882
11	-90.817547	-90.817413	-90.818307	-90.823507	-90.841890
12	-90.817648	-90.817586	-90.818459	-90.823633	-90.841958
13	-90.817395	-90.816509	-90.817584	-90.822979	-90.841966

- 1.** STO-6G//MCSCF(66 CSFs); **2.** STO-6G//MCSCF(196 CSFs);
3. STO-6G//MCSCF(1176 CSFs); **4.** STO-6G//MCSCF(5292 CSFs);
5. STO-6G//MCSCF(19404 CSFs);
6. 6-31G//MCSCF(66 CSFs); **7.** 6-31G//MCSCF(196 CSFs);
8. 6-31G//MCSCF(1176 CSFs); **9.** 6-31G//MCSCF(5292 CSFs);
10. 6-31G//MCSCF(19404 CSFs);
11. 6-31G*//MCSCF(196 CSFs); **12.** 6-31G*//MCSCF(1176 CSFs);
13. 6-31G*//MCSCF(5292 CSFs);

Table 15. Moller-Plesset Energies For Planar-Bridged C_2Li_2

Model	Energy (a.u.)				
	MP2	MP3	MP4DQ	MP4SDQ	MP4SDTQ
1	-90.482873	-90.474074	-90.481409	-90.485066	-90.493219
2	-90.486556	-90.477576	-90.485061	-90.488453	-90.496212
3	-90.486334	-90.477583	-90.484954	-90.488358	-90.496113
4	-90.486312	-90.477497	-90.484885	-90.488332	-90.496162
5	-90.486488	-90.477571	-90.485003	-90.488456	-90.496308
6	-90.707642	-90.698047	-90.705017	-90.709181	-90.721030
7	-90.707557	-90.697762	-90.704818	-90.709009	-90.720929
8	-90.709531	-90.700095	-90.706996	-90.711168	-90.723015
9	-90.711046	-90.701598	-90.708500	-90.712701	-90.724604
10	-90.710872	-90.701297	-90.708253	-90.712467	-90.724411
11	-90.832879	-90.833521	-90.834449	-90.839239	-90.857385
12	-90.832647	-90.833446	-90.834302	-90.839059	-90.857123
13	-90.832275	-90.833011	-90.833863	-90.838645	-90.856776

- 1.** STO-6G//MCSCF(66 CSFs); **2.** STO-6G//MCSCF(196 CSFs);
3. STO-6G//MCSCF(1176 CSFs); **4.** STO-6G//MCSCF(5292 CSFs);
5. STO-6G//MCSCF(19404 CSFs);
6. 6-31G//MCSCF(66 CSFs); **7.** 6-31G//MCSCF(196 CSFs);
8. 6-31G//MCSCF(1176 CSFs); **9.** 6-31G//MCSCF(5292 CSFs);
10. 6-31G//MCSCF(19404 CSFs);
11. 6-31G*//MCSCF(196 CSFs); **12.** 6-31G*//MCSCF(1176 CSFs);
13. 6-31G*//MCSCF(5292 CSFs);

Table 16. Moller-Plesset Relative Energies For C₂Li₂

Model	ΔE^\dagger <i>Linear-Bridged</i>				
	MP2	MP3	MP4DQ	MP4SDQ	MP4SDTQ
1	9.8	11.5	11.2	12.9	13.2
2	11.7	13.6	13.3	14.8	14.8
3	11.6	13.6	13.2	14.7	14.7
4	10.7	13.5	12.8	14.4	14.2
5	10.6	13.6	12.9	14.4	14.2
6	-5.2	-7.7	-6.4	-6.1	-5.6
7	-5.4	-7.9	-6.6	-6.3	-5.8
8	-5.0	-7.2	-6.0	-5.8	-5.4
9	-4.8	-6.6	-5.6	-5.4	-5.2
10	-5.0	-6.7	-5.7	-5.5	-5.3
11	9.6	10.1	10.1	9.9	9.7
12	9.4	10.0	9.9	9.7	9.5
13	9.3	10.4	10.2	9.8	9.3

† in kcal/mol units

1. STO-6G//MCSCF(66 CSFs); 2. STO-6G//MCSCF(196 CSFs);
3. STO-6G//MCSCF(1176 CSFs); 4. STO-6G//MCSCF(5292 CSFs);
5. STO-6G//MCSCF(19404 CSFs);
6. 6-31G//MCSCF(66 CSFs); 7. 6-31G//MCSCF(196 CSFs);
8. 6-31G//MCSCF(1176 CSFs); 9. 6-31G//MCSCF(5292 CSFs);
10. 6-31G//MCSCF(19404 CSFs);
11. 6-31G*//MCSCF(196 CSFs); 12. 6-31G*//MCSCF(1176 CSFs);
13. 6-31G*//MCSCF(5292 CSFs);

3.2 Dilithiomethane

3.2.1 Hartree-Fock (RHF, UHF, ROHF) Calculations

Starting at the standard geometries 7 – 9 in Figure 1, the Hartree-Fock restricted (RHF), unrestricted (UHF) and open shell restricted (ROHF) geometry optimization were carried out on each of the three forms and led to two different symmetries for each: one is for the singlet state which resulted from the RHF optimization, the other from both the UHF and ROHF optimizations. The Hartree-Fock geometry optimizations were carried out within the assumed standard geometry with STO-6G, 6-31G (but not for UHF), Dunning-Hay (9s 5p)/[4s 2p], 6-31G* and 6-31G** basis sets.

The Hartree-Fock energies for the geometry optimized CH_2Li_2 form are included in Table 17. The relative Hartree-Fock energies among three symmetries, but within the same theoretical model, are listed in Table 18. The relative Hartree-Fock energies of the singlet state vs. the triplet state within the same symmetry are given in Table 19. With all basis sets used in this work, the Hartree-Fock energy of the tetrahedral CH_2Li_2 (C_{2v}) is always the lowest while that of the transplanar form is the highest for both the singlet and the triplet states. Within the same symmetry, the Hartree-Fock energy of the triplet state is always lower relative to the singlet except with the minimal

Table 17. Singlet and Triplet HF Energies For CH₂Li₂

Method	Energy (a.u.)		
	Tetra	Cis-planar	Trans-planar
RHF/STO-6G	-53.683524	-53.660360	-53.599967
RHF/6-31G	-53.820860	-53.808334	-53.752104
RHF/D95V	-53.825441	-53.818013	-53.760191
RHF/6-31G*	-53.830163	-53.820650	-53.759979
RHF/6-31G**	-53.834654	-53.825404	-53.767306
UHF/STO-6G	-53.654154	-53.640889	-53.597938
UHF/6-31G	-53.847344	-53.843632	-53.770301
UHF/D95V	-53.853047	-53.850712	-53.766440
UHF/6-31G*	-53.860654	-53.856875	-53.778837
UHF/6-31G**	-53.864283	-53.860691	-53.784728
ROHF/STO-6G	-53.701280	-53.686580	-53.593329
ROHF/D95V	-53.851045	-53.848727	-53.774497
ROHF/6-31G*	-53.857031	-53.853532	-53.776743
ROHF/6-31G**	-53.860708	-53.857391	-53.781102

† RHF for singlet
‡ UHF and ROHF for triplet

Table 18. Singlet and Triplet HF Relative Energies For CH₂Li₂

Method	ΔE^\dagger		
	Tetra	Cis-planar	Trans-planar
RHF/STO-6G	0.0	14.5	52.4
RHF/6-31G	0.0	7.9	43.1
RHF/D95V	0.0	4.7	40.9
RHF/6-31G*	0.0	6.0	44.0
RHF/6-31G**	0.0	5.8	42.3
UHF/STO-6G	0.0	8.3	35.3
UHF/6-31G	0.0	2.3	48.3
UHF/D95V	0.0	1.4	54.3
UHF/6-31G*	0.0	2.4	51.3
UHF/6-31G**	0.0	2.3	49.9
ROHF/STO-6G	0.0	9.2	67.7
ROHF/D95V	0.0	1.5	48.0
ROHF/6-31G*	0.0	2.2	50.4
ROHF/6-31G**	0.0	2.1	50.0

[†] within the same method, in kcal/mol unit

Table 19. Singlet and Triplet HF Relative Energies For CH₂Li₂ (2)

Method	ΔE^\dagger		
	Tetra	Cis-planar	Trans-planar
RHF/STO-6G	113.4	125.7	115.9
RHF/6-31G	27.2	32.9	20.5
RHF/D95V	24.4	26.9	15.4
RHF/6-31G*	21.4	25.1	15.5
RHF/6-31G**	18.6	22.1	10.9
UHF/STO-6G	131.9	137.9	117.2
UHF/6-31G	10.6	10.7	9.1
UHF/D95V	7.1	6.3	11.5
UHF/6-31G*	2.3	2.4	3.7
UHF/6-31G**	0.0	0.0	0.0
ROHF/STO-6G	102.3	109.3	120.1
ROHF/D95V	8.3	7.5	6.4
ROHF/6-31G*	4.6	4.6	5.0
ROHF/6-31G**	2.2	2.1	2.3

[†] within the same symmetry, in kcal/mol unit

STO-6G basis. Furthermore, the UHF wavefunction generally yielded lower energy than did the corresponding ROHF wavefunction.

The Hartree-Fock optimized geometries for all basis sets are provided in Tables 20 – 22. It was found that the singlet and triplet states do have quite different structures except for the case of the trans planar D_{2h} CH_2Li_2 . In the case of the tetrahedral C_{2v} form, the bond length of C—Li in the triplet state is longer than that in the singlet state by about 0.1 Å but the distance of Li—Li in the former is shorter than that in the latter by almost 1 Å. Accordingly, the bond angle of H—C—Li in the triplet state is greater than that in the singlet state by around 10 degrees while the Li—C—Li bond angle is smaller by a range of 40 to 50 degrees. A similar trend of change in bond lengths and bond angles was also found in the cis planar C_{2v} CH_2Li_2 but the Li—C—Li angle is smaller by about 30 degrees. For the case of the trans planar D_{2h} CH_2Li_2 , the bond length of C—Li in the triplet state is longer than that in the singlet state by about 0.2 Å, and the internuclear distance between the two lithium atoms is shorter, – not longer as found in the tetrahedral and cis planar CH_2Li_2 , – by about 0.4 Å. The Mulliken net charges, as well as the dipole moments for the three forms of CH_2Li_2 , are given in Tables 23 – 25. In all cases except for the STO-6G basis set, the carbon atom is always negatively charged, and the hydrogen and lithium atoms positively charged. The dipole moment for the singlet and triplet states of CH_2Li_2 with C_{2v} symmetry changed drastically from around 5 Debyes in the singlet to

Table 20-1. HF Optimized Geometries For CH₂Li₂(tetra C_{2v})

Method	Internuclear Distances (Å)				
	C—H	C—Li	H—H	Li—Li	H—Li
RHF/STO-6G	1.085	1.921	1.744	3.311	2.475
RHF/6-31G	1.101	1.970	1.789	3.321	2.542
RHF/D95V	1.102	1.983	1.795	3.340	2.552
RHF/6-31G*	1.100	1.974	1.769	3.399	2.533
RHF/6-31G**	1.100	1.972	1.769	3.399	2.531
UHF/STO-6G	1.086	2.032	1.730	3.066	2.657
UHF/6-31G	1.094	2.102	1.767	2.492	2.793
UHF/D95V	1.096	2.128	1.768	2.516	2.820
UHF/6-31G*	1.093	2.107	1.749	2.486	2.800
UHF/6-31G**	1.093	2.107	1.749	2.486	2.803
ROHF/STO-6G	1.085	2.043	1.724	2.292	2.752
ROHF/D95V	1.095	2.127	1.767	2.507	2.820
ROHF/6-31G*	1.092	2.107	1.748	2.485	2.804
ROHF/6-31G**	1.092	2.107	1.748	2.485	2.804

Table 20.2. HF Optimized Geometries For CH₂Li₂

(tetra C_{2v})

Method	Bond Angles (°)		
	H-C-H	H-C-Li	Li-C-Li
RHF/STO-6G	106.9	107.4	119.6
RHF/6-31G	108.5	108.4	114.9
RHF/D95V	109.0	110.0	114.8
RHF/6-31G*	107.1	107.4	119.0
RHF/6-31G**	107.2	107.4	119.0
UHF/STO-6G	105.6	113.4	97.9
UHF/6-31G	107.6	118.4	72.7
UHF/D95V	107.6	118.5	72.5
UHF/6-31G*	106.3	118.9	72.3
UHF/6-31G**	106.3	118.9	72.3
ROHF/STO-6G	105.2	120.0	68.3
ROHF/D95V	107.5	118.6	72.2
ROHF/6-31G*	106.3	119.0	72.3
ROHF/6-31G**	106.3	119.1	72.3

Table 21.1. HF Optimized Geometries For CH₂Li₂

(cis C_{2v})

Method	Internuclear Distances (Å)				
	C—H	C—Li	H—H	Li—Li	H—Li
RHF/STO-6G	1.104	1.737	1.713	2.626	1.890
RHF/6-31G	1.102	1.846	1.725	2.796	1.965
RHF/D95V	1.102	1.857	1.726	2.823	1.971
RHF/6-31G*	1.100	1.837	1.716	2.832	1.940
RHF/6-31G**	1.100	1.835	1.715	2.841	1.934
UHF/STO-6G	1.095	1.972	1.699	2.941	2.099
UHF/6-31G	1.097	2.060	1.737	2.453	2.353
UHF/D95V	1.097	2.085	1.737	2.472	2.381
UHF/6-31G*	1.095	2.058	1.723	2.451	2.359
UHF/6-31G**	1.095	2.058	1.723	2.451	2.359
ROHF/STO-6G	1.092	1.984	1.704	2.241	2.321
ROHF/D95V	1.097	2.082	1.737	2.467	2.375
ROHF/6-31G*	1.094	2.055	1.720	2.444	2.357
ROHF/6-31G**	1.094	2.055	1.720	2.444	2.357

Table 21.2. HF Optimized Geometries For CH_2Li_2
(cis C_{2v})

Method	Bond Angles ($^\circ$)		
	H-C-H	H-C-Li	Li-C-Li
RHF/STO-6G	101.7	80.0	98.2
RHF/6-31G	103.0	79.2	98.5
RHF/D95V	103.1	79.0	98.9
RHF/6-31G*	102.5	78.3	100.9
RHF/6-31G**	102.4	78.1	101.4
UHF/STO-6G	101.8	80.9	96.4
UHF/6-31G	104.6	91.1	73.1
UHF/D95V	104.7	91.1	72.7
UHF/6-31G*	103.7	91.6	73.1
UHF/6-31G**	103.6	91.6	73.0
ROHF/STO-6G	102.2	94.5	68.8
ROHF/D95V	104.7	91.5	72.7
ROHF/6-31G*	103.6	91.6	73.0
ROHF/6-31G**	103.6	91.6	73.0

Table 22. HF Optimized Geometries For CH_2Li_2

(trans D_{2h})

Method	Internuclear Distances (\AA)				
	C—H	C—Li	H—H	Li—Li	H—Li
RHF/STO-6G	1.067	1.804	2.135	3.608	2.096
RHF/6-31G	1.067	1.943	2.134	3.886	2.217
RHF/D95V	1.069	1.957	2.137	3.914	2.230
RHF/6-31G*	1.065	1.936	2.131	3.872	2.210
RHF/6-31G**	1.064	1.934	2.128	3.868	2.208
UHF/STO-6G	1.069	2.009	2.137	4.019	2.276
UHF/6-31G	1.065	2.118	2.129	4.237	2.371
UHF/D95V	1.067	2.150	2.134	4.300	2.400
UHF/6-31G*	1.063	2.117	2.126	4.235	2.369
UHF/6-31G**	1.064	2.117	2.129	4.234	2.370
ROHF/STO-6G	1.066	2.000	2.132	3.997	2.265
ROHF/D95V	1.065	2.144	2.129	4.288	2.393
ROHF/6-31G*	1.062	2.130	2.124	4.260	2.331
ROHF/6-31G**	1.061	2.105	2.124	4.209	2.357

Table 23. Mulliken Net Charges and Dipole Moments

For CH_2Li_2 (tetra C_{2v})

Method	Net Charge			Dipole Moment (Debye)
	C	H	Li	
RHF/STO-6G	-0.20	0.03	0.07	3.3096
RHF/6-31G	-0.87	0.10	0.33	5.4244
RHF/D95V	-1.13	0.14	0.43	5.6473
RHF/6-31G*	-0.77	0.12	0.26	5.1853
RHF/6-31G**	-0.65	0.08	0.25	5.1841
UHF/STO-6G	-0.20	0.04	0.06	0.2723
UHF/6-31G	-0.76	0.13	0.25	1.0678
UHF/D95V	-0.90	0.14	0.31	0.9857
UHF/6-31G*	-0.68	0.14	0.20	1.0732
UHF/6-31G**	-0.58	0.09	0.20	1.0620
ROHF/STO-6G	-0.19	0.03	0.07	1.0215
ROHF/D95V	-0.90	0.14	0.31	0.9542
ROHF/6-31G*	-0.69	0.15	0.20	1.0540
ROHF/6-31G**	-0.58	0.09	0.20	1.0432

Table 24. Mulliken Net Charges and Dipole Moments

For CH₂Li₂ (cis C_{2v})

Method	Net Charge			Dipole Moment
	C	H	Li	(Debye)
RHF/STO-6G	-0.26	0.04	0.09	1.8201
RHF/6-31G	-0.86	0.08	0.35	4.4877
RHF/D95V	-0.96	0.13	0.41	5.0556
RHF/6-31G*	-0.69	0.13	0.22	4.3164
RHF/6-31G**	-0.58	0.07	0.22	4.3015
UHF/STO-6G	-0.22(0.40)	0.04(-0.03)	0.07(0.12)	1.1692
UHF/6-31G	-0.76(0.24)	0.10(-0.03)	0.28(0.06)	1.4001
UHF/D95V	-0.84(0.23)	0.11(-0.02)	0.31(0.05)	1.2083
UHF/6-31G*	-0.68(0.21)	0.14(-0.02)	0.20(0.06)	1.4596
UHF/6-31G**	-0.56(0.21)	0.08(-0.02)	0.20(0.06)	1.4430
ROHF/STO-6G	-0.22(0.04)	0.08(0.00)	0.03(0.13)	1.5512
ROHF/D95V	-0.84(0.04)	0.11(0.00)	0.31(0.06)	1.2190
ROHF/6-31G*	-0.68(0.04)	0.14(0.00)	0.20(0.06)	1.4957
ROHF/6-31G**	-0.57(0.04)	0.09(0.00)	0.20(0.06)	1.4847

Table 25. Mulliken Net Charges and Dipole Moments

For CH₂Li₂ (trans C_{2v})

Method	Net Charge			Dipole Moment (Debye)
	C	H	Li	
RHF/STO-6G	-0.34	0.15	0.02	0.0000
RHF/6-31G	-1.09	0.26	0.29	0.0000
RHF/D95V	-1.33	0.28	0.39	0.0000
RHF/6-31G*	-0.92	0.27	0.19	0.0000
RHF/6-31G**	-0.79	0.23	0.12	0.0000
UHF/STO-6G	-0.29(0.43)	0.14(-0.04)	0.01(0.09)	0.0009
UHF/6-31G	-0.94(0.27)	0.27(-0.03)	0.20(0.08)	0.0125
UHF/D95V	-1.16(0.25)	0.28(-0.03)	0.29(0.02)	0.0010
UHF/6-31G*	-0.85(0.25)	0.28(-0.03)	0.14(0.08)	0.0140
UHF/6-31G**	-0.64(0.25)	0.20(-0.03)	0.12(0.09)	0.0001
ROHF/STO-6G	-0.30(0.00)	0.14(0.00)	0.01(0.10)	0.0293
ROHF/D95V	-1.14(0.05)	0.30(0.00)	0.27(0.06)	0.0635
ROHF/6-31G*	-0.85(0.03)	0.28(0.00)	0.20(0.07)	?
ROHF/6-31G**	-0.72(0.05)	0.24(0.00)	0.13(0.06)	0.0016

1 to 1.5 Debyes in the triplet state. Due to the D_{2h} symmetry, the trans planar form of CH_2Li_2 shows a zero value of the dipole moment in both the singlet and triplet state. The total overlap populations in Tables 26, 27 and 28 show that the accumulation of charge between two lithium atoms increases with the decrease in the Li-C-Li bond angle.

3.2.2 MCSCF-CASSCF Calculations

The MCSCF-CASSCF calculations were carried out with three types of basis sets: the Dunning-Hay contracted (9s 5p)/[4s 2p], 6-31G* and 6-31G**. For all three types of symmetry of the singlet state, the complete active space consisted of

- 3 inactive orbitals
- 8 active orbitals

while for the triplet state it was

- 3 inactive orbitals
- 9 active orbitals

For the latter case, the active subspace was constructed in the sense of the spin-unrestricted consideration, that is, electrons with different spin were assigned to different spatial orbitals.

Table 26. Mulliken Overlap Analyses For CH₂Li₂
(tetra C_{2v})

Method	Overlap Population				
	C—H	C—Li	H—H	Li—Li	H—Li
RHF/STO-6G	0.74	0.66	-0.04	-0.27	-0.05
RHF/6-31G	0.68	0.67	-0.08	-0.29	-0.04
RHF/D95V	0.68	0.66	-0.08	-0.26	-0.04
RHF/6-31G*	0.68	0.74	-0.08	-0.29	-0.04
RHF/6-31G**	0.70	0.74	-0.08	-0.30	-0.04
UHF/STO-6G	0.75	0.43	-0.05	0.00	-0.05
UHF/6-31G	0.70	0.30	-0.08	0.27	-0.02
UHF/D95V	0.67	0.22	-0.07	0.46	-0.03
UHF/6-31G*	0.72	0.38	-0.07	0.28	-0.03
UHF/6-31G**	0.74	0.38	-0.07	0.27	-0.03
ROHF/STO-6G	0.76	0.44	-0.05	0.25	-0.05
ROHF/D95V	0.68	0.22	-0.07	0.46	-0.03
ROHF/6-31G*	0.72	0.38	-0.08	0.25	-0.03
ROHF/6-31G**	0.75	0.38	-0.08	0.24	-0.03

Table 27. Mulliken Overlap Analyses For CH₂Li₂

(cis C_{2v})

Method	Overlap Population				
	C—H	C—Li	H—H	Li—Li	H—Li
RHF/STO-6G	0.69	0.61	-0.03	0.30	0.06 -0.09
RHF/6-31G	0.62	0.64	-0.03	0.22	0.01 -0.05
RHF/D95V	0.56	0.67	-0.03	0.17	0.00 -0.08
RHF/6-31G*	0.61	0.77	-0.01	0.27	0.00 -0.09
RHF/6-31G**	0.62	0.77	-0.00	0.27	0.00 -0.08
UHF/STO-6G	0.71	0.41	-0.04	0.10	0.00 -0.07
UHF/6-31G	0.68	0.27	-0.05	0.42	0.00 -0.04
UHF/D95V	0.65	0.21	-0.05	0.45	-0.01 -0.04
UHF/6-31G*	0.67	0.37	-0.04	0.46	0.00 -0.04
UHF/6-31G**	0.65	0.37	-0.04	0.46	0.00 -0.05
ROHF/STO-6G	0.36	0.18	-0.02	0.03	0.00 -0.03
ROHF/D95V	0.66	0.21	-0.05	0.45	0.00 -0.03
ROHF/6-31G*	0.68	0.38	-0.04	0.46	0.00 -0.04
ROHF/6-31G**	0.70	0.38	-0.04	0.46	0.00 -0.04

Table 28. Mulliken Overlap Analyses For CH₂Li₂

(trans D_{2h})

Method	Overlap Population				
	C—H	C—Li	H—H	Li—Li	H—Li
RHF/STO-6G	0.72	0.64	-0.03	-0.44	0.04
RHF/6-31G	0.70	0.64	-0.04	0.00	0.03
RHF/D95V	0.70	0.64	-0.03	-0.05	0.02
RHF/6-31G*	0.66	0.75	-0.04	-0.03	0.04
RHF/6-31G**	0.70	0.74	-0.05	-0.03	0.05
UHF/STO-6G	0.73	0.41	-0.03	-0.31	0.02
UHF/6-31G	0.71	0.30	-0.02	0.03	0.01
UHF/D95V	0.71	0.23	-0.03	0.13	0.01
UHF/6-31G*	0.69	0.37	-0.03	0.04	0.02
UHF/6-31G**	0.65	0.37	-0.04	0.03	0.02
ROHF/STO-6G	0.65	0.42	-0.03	-0.31	0.02
ROHF/D95V	0.73	0.23	-0.03	0.07	0.00
ROHF/6-31G*	0.71	0.26	-0.03	0.02	0.03
ROHF/6-31G**	0.74	0.38	-0.04	0.04	0.02

The MCSCF optimized energies are presented in Tables 29 – 30. Tables 31 and 32 show the MCSCF optimized geometries. It can be seen from these that there is a drastic change in bond angles. For both the tetrahedral and cis planar forms, the bond angle of Li–C–Li in the triplet state is much smaller than that in the singlet state by more than 50 degrees while the H–C–Li bond angle in the triplet state is larger than that in the singlet state. The latter difference is not very large: 10 to 13 degrees. In terms of the bond length, lengthening of the C—Li and H—Li and shortening of Li—Li is observed in the triplet state for both the tetrahedral C_{2v} and cis planar C_{2v} forms. For the case of the trans planar D_{2h} form, lengthening of the C—Li, H—Li as well as Li—Li distances is found in the triplet state. The Mulliken overlap population analysis in Table 33 confirms the changes in geometries described above. The C—Li and Li—Li overlap population changes accordingly. It was found that there is an obvious accumulation of positive charge between two lithium atoms in the triplet state for the tetrahedral and cis planar CH_2Li_2 . The Mulliken net charge and dipole moment are included in Table 34. This shows that the singlet state is more polarized than the triplet state.

Tables 35 – 37 provide the coefficients of the first three most important configurations in each of these wavefunctions. For the case of all singlet states, the ground state configuration has the largest coefficient and thus is dominant in the MCSCF wavefunction. For the case of the triplet states, the contributions to the MCSCF wave

Table 29. Singlet and Triplet MCSCF Energies For CH₂Li₂

Singlet			
Method	Tetra	Cis-planar	Trans-planar
MCSCF/D95V	-53.927323	-53.920768	-53.819658
MCSCF/6-31G*	-53.930761	-53.921600	-53.825164
MCSCF/6-31G**	-53.934920	-53.926007	-53.832463

Triplet			
Method	Tetra	Cis-planar	trans-planar
MCSCF/D95V	-53.926215	-53.924066	-53.842219
MCSCF/6-31G8	-53.931691	-53.927742	-53.845785
MCSCF/6-31G**	-53.934978	-53.931207	-53.849954

Table 30. MCSCF Relative Energies For CH₂Li₂ (kcal/mol)

Basis	Singlet			Triplet		
	Tetra	Cis	Trans	Tetra	Cis	Trans
D95V	0.0	4.1	67.6	0.7	2.0	53.4
6-1G*	0.6	6.3	66.8	0.0	2.5	53.9
6-31G**	0.04	5.6	64.3	0.0	2.4	53.3

Table 31. MCSCF Optimized Geometries For CH₂Li₂

Symmetry	Basis	Multiplicity	Internuclear Distances (Å)				
			C—H	C—Li	H—H	Li—Li	H—Li
Tetra	D95V	Sing.	1.123	2.020	1.839	3.348	2.607
	6-31G*	Sing.	1.116	2.011	1.813	3.379	2.590
	6-31G**	Sing.	1.115	2.008	1.813	3.375	2.589
	D95V	Trip.	1.123	2.162	1.808	2.530	2.874
	6-31G*	Trip.	1.114	2.139	1.785	2.502	2.851
	6-31G**	Trip.	1.114	2.139	1.783	2.501	2.850
Cis	D95V	Sing.	1.125	1.887	1.783	2.814	2.014
	6-31G*	Sing.	1.119	1.871	1.770	2.810	1.976 2.999
	6-31G**	Sing.	1.118	1.867	1.768	2.825	1.978 2.985
	D95V	Trip.	1.125	2.106	1.777	2.485	2.416 3.202
	6-31G*	Trip.	1.117	2.081	1.758	2.456	2.396 3.171
	6-31G**	Trip.	1.116	2.082	1.756	2.458	2.395 3.170
Trans	D95V	Sing.	1.091	1.964	2.182	3.927	2.246
	6-31G*	Sing.	1.084	1.938	2.168	3.876	2.220
	6-31G**	Sing.	1.082	1.933	2.164	3.867	2.216
	D95V	Trip.	1.089	2.159	2.178	4.410	2.417
	6-31G*	Trip.	1.084	2.110	2.167	4.314	2.414
	6-31G**	Trip.	1.081	2.130	2.164	4.260	2.389

Table 32. MCSCF Optimized Geometries For CH₂Li₂ (Part 2)

Symmetry	Basis	Multiplicity	Bond Angle (°)		
			H—C—H	H—C—Li	Li—C—Li
Tetra	D95V	Sing.	109.9	108.8	111.9
	6-31G*	Sing.	108.8	108.5	114.4
	6-31G**	Sing.	107.3	108.6	114.4
	D95V	Trip.	107.3	118.6	71.6
	6-31G*	Trip.	106.4	119.0	71.6
	6-31G**	Trip.	106.3	119.0	71.6
Cis	D95V	Sing.	104.9	79.1	96.5
	6-31G*	Sing.	104.6	79.2	97.4
	6-31G**	Sing.	104.5	78.5	98.3
	D95V	Trip.	104.4	91.7	72.3
	6-31G*	Trip.	103.9	91.8	72.3
	6-31G**	Trip.	103.7	91.6	72.4

Table 33. Mulliken MCSCF Overlap Analyses For CH₂Li₂

Symmetry	Basis	Multiplicity	Overlap Population (Å)				
			C—H	C—Li	H—H	Li—Li	H—Li
Tetra	D95V	Sing.	0.65	0.63	-0.08	-0.32	-0.04
	6-31G*	Sing.	0.65	0.67	-0.08	-0.33	-0.04
	6-31G**	Sing.	0.67	0.67	-0.08	-0.35	-0.04
	D95V	Trip.	0.64	0.25	-0.08	0.45	-0.03
	6-31G*	Trip.	0.67	0.39	-0.08	0.17	-0.03
	6-31G**	Trip.	0.69	0.39	-0.08	0.16	-0.03
Cis	D95V	Sing.	0.55	0.65	-0.03	0.25	-0.09 0.00
	6-31G*	Sing.	0.58	0.71	-0.01	0.35	-0.07 0.00
	6-31G**	Sing.	0.59	0.71	-0.01	0.35	-0.07 0.00
	D95V	Trip.	0.61	0.25	-0.05	0.47	-0.04 -0.01
	6-31G*	Trip.	0.63	0.40	-0.04	0.48	-0.04 -0.01
	6-31G**	Trip.	0.65	0.40	-0.04	0.48	-0.04 -0.01
Trans	D95V	Sing.	0.65	0.63	-0.04	-0.13	0.03
	6-31G*	Sing.	0.62	0.73	-0.05	-0.08	0.04
	6-31G**	Sing.	0.65	0.73	-0.05	-0.08	0.05
	D95V	Trip.	0.68	0.25	-0.03	0.05	-0.01
	6-31G*	Trip.	0.67	0.35	-0.03	0.00	0.02
	6-31G**	Trip.	0.69	0.35	-0.04	0.01	0.02

Table 34. Mulliken MCSCF Net Charges For CH₂Li₂

Symmetry	Basis	Multiplicity	Overlap Population (Å)			Dipole Moment (Debye)
			C	H	Li	
Tetra	D95V	Sing.	-0.90	0.11	0.34	5.2231
	6-31G*	Sing.	-0.59	0.10	0.20	4.9348
	6-31G**	Sing.	-0.48	0.05	0.19	4.9553
	D95V	Trip.	-0.77	0.11	0.27	0.9344
	6-31G*	Trip.	-0.56	0.11	0.17	1.0447
	6-31G**	Trip.	-0.47	0.11	0.17	1.0130
Cis	D95V	Sing.	-0.76	0.04	0.34	4.4215
	6-31G*	Sing.	-0.50	0.16	0.09	3.7945
	6-31G**	Sing.	-0.43	0.05	0.16	3.7887
	D95V	Trip.	-0.72	0.08	0.28	1.2657
	6-31G*	Trip.	-0.56	0.11	0.17	1.5444
	6-31G**	Trip.	-0.46	0.06	0.17	1.5194
Trans	D95V	Sing.	-1.18	0.23	0.34	0.0000
	6-31G*	Sing.	-0.80	0.23	0.17	0.0000
	6-31G**	Sing.	-0.70	0.18	0.17	0.0000
	D95V	Trip.	-0.96	0.25	0.23	0.0000
	6-31G*	Trip.	-0.73	0.24	0.12	0.0000
	6-31G**	Trip.	-0.62	0.20	0.11	0.0000

Table 35. The First Three Most Important CSFs
in the MCSCF Wavefunction For tetra CH_2Li_2

Basis	Singlet			Triplet		
	First	Second	Third	First	Second	Third
D95V	0.96	0.11	0.10	0.54	0.54	0.42
6-31G*	0.96	0.11	0.10	0.55	0.52	0.45
6-31G**	0.96	0.11	0.10	0.54	0.54	0.43

Table 36. The First Three Most Important CSFs
in the MCSCF Wavefunction For cis CH_2Li_2

Basis	Singlet			Triplet		
	First	Second	Third	First	Second	Third
D95V	0.96	0.07	0.07	0.78	0.58	0.05
6-31G*	0.96	0.13	0.08	0.76	0.61	0.04
6-31G**	0.96	0.12	0.08	0.74	0.64	0.04

Table 37. The First Three Most Important CSFs ex
in the MCSCF Wavefunction For trans CH₂Li₂

Basis	Singlet			Triplet		
	First	Second	Third	First	Second	Third
D95V	0.98	0.10	0.07	0.91	0.29	0.11
6-31G*	0.98	0.10	0.07	0.97	0.07	0.07
6-31G**	0.98	0.10	0.07	0.98	0.09	0.06

functions from these three most important configurations – especially from the first two in the tetrahedral C_{2v} and the cis planar C_{2v} forms – are rather close. The obvious trend is that the bigger the contribution from highly excited states the lower is the energy of the MCSCF wavefunction.

3.2.3 CISD Calculations

With all, not just valence, electrons included in a correlation energy, CISD/6-31G* geometry optimization calculations show that for the three forms of the singlet states of the dilithiomethane molecule the tetrahedral-like C_{2v} structure is the lowest in energy, then the cis planar C_{2v} is 4.5 kcal/mol above the former, the trans planar D_{2h} form again is the most unfavorable in energy, by 45 kcal/mol higher than the lowest one.

Chapter 4

Discussion

4.1 Dilithioacetylene

4.1.1 Hartree-Fock Structures

The Hartree-Fock optimized (equilibrium) structures for linear C_2Li_2 with all basis sets employed are in close accord. The change in the C—C and C—Li bond lengths, if any, does not exceed 0.1 Å. For the planar bridged structure, the C—C bond length is insensitive to the basis set. The Li—Li distance is quite short (3.59 Å) with the minimal STO-6G basis but much longer (3.95 Å) with the Dunning-Hay (9s 5p)/[3s 2p] basis. In both forms of C_2Li_2 , the RHF/6-311G equilibrium structures are identical to those obtained with the 6-31G* representation.

The Hartree-Fock results suggest that the presence of *p* and *d* functions on lithium atoms (unoccupied in the free atom) has little effect on the C—C skeleton of the planar bridged structure of dilithioacety-

lene molecule over the linear form. The C—Li distance in the former, [1.904 Å with STO-6G and 2.072 Å with D95V (Dunning-Hay basis)], is significantly longer than that in the linear alternative which is 1.811 Å with STO-6G and 1.903 Å with D95V basis.

The Hartree-Fock optimized energies for both the linear and planar bridged forms of dilithioacetylene are basis set dependent. The addition of *d* functions plays an important role in stabilizing the bridged structure of C₂Li₂. The mechanism through which the *d* functions affect the stability of dilithioacetylene molecule might also be the so-called “Basis Set Superposition Effect” (BSSE) [77,31]. For the C₂Li₂ molecule, the lithium atom is an electron-deficient element and does not contain any 2*p* electron in the ground state. In the 6-31G* basis representation, six *d* functions are assigned to each of four atoms including lithium in addition to 2*p* functions which are unoccupied in lithium atom. Therefore, the 2*p* electrons of carbon atoms are able to “borrow” excess basis functions from lithium. In other words, the *d* functions of lithium atoms could extend into the vicinity of carbon atoms. This leads to a lowering of the energy of the C₂Li₂ molecule. Due to the D_{2h} symmetry of the planar bridged form, each carbon atom is directly interacting with two lithium atoms, not one as in the linear form of C₂Li₂. Thus, it is altogether natural that the bridged structure would benefit more from extra *d* functions of lithium than does the linear one. In this work, the *d* function superposition effect (DFSE) is examined. Both the planar bridged and linear form of di-

lithioacetylene are calculated with a modified 6-31G* basis in which there are no *d* functions assigned to lithium atoms. The energy gain due to the *d* function superposition effect, ΔE_{DFSE} , is defined as

$$\Delta E = E_{(6-31G^*)_1} - E_{(6-31G^*)_2} \quad (4.1)$$

where $E_{(6-31G^*)_1}$ is the RHF energy with the conventional 6-31G* basis set (the RHF/6-31G* energy listed in Table 2), and $E_{(6-31G^*)_2}$ is the energy obtained with the modified 6-31G* basis described above. Table 38 shows clearly the following result

$$(\Delta E_{DFSE})_{Bridged} > (\Delta E_{DFSE})_{linear} \quad (4.2)$$

If ΔE_{DFSE} is subtracted from the RHF/6-31G* in Table 2, the difference between the linear and planar bridged form of C_2Li_2 would be reduced to 3.7 kcal/mol. The *d* function superposition effect (DFSE) implies that for an electron-deficient element such as lithium the Hartree-Fock calculation with *d* function-augmented basis set should have this effect taken into account. Accordingly, among other things, the RHF geometry for these types of molecules might not be very reliable.

4.1.2 MCSCF Structures

Compared with the RHF optimized structures of C_2Li_2 (see Table 3), the multiconfiguration CASSCF geometry optimization generally

Table 38. The *d* Function Superposition Effect (DFSE)

For C_2Li_2

	Linear $D_{\infty h}$			Planar Bridged D_{2h}		
	(6-31G*) ₁	(6-31G*) ₂	ΔE_{DFSE}^3	(6-31G*) ₁	(6-31G*) ₂	ΔE_{DFSE}^3
RHF	-90.550953	-90.548765	0.7	-90.561614	-90.555682	3.7

1 The conventional 6-31G* basis

2 The 6-31G* basis without the *d* functions for lithium

3 in kcal/mol

leads to an increase in the C—C bond length in the range of ca. 0.2 – 0.5 Å for dilithioacetylene molecules (see Table 7).

The general structure of the electron correlation effect can be deduced from Table 39 which shows the occupation numbers of the active orbitals in MCSCF wavefunctions. Adding together the occupation numbers for each row, which corresponds to an active subspace, gives a number very close to 10; the number of the valence electrons in C_2Li_2 . Therefore, an overall description of the MCSCF-CASSCF wavefunction can hardly be written in terms of doubly-occupied orbitals. It can be seen that the increase in the optimized C—C bond lengths of the linear structure of C_2Li_2 (see Table 7) is accompanied by a decrease in the occupation numbers of the $1\pi_u$ orbital. That number is 3.886 in the 196 CFSs space and reduced to 3.867 in the 19404 CFSs space with STO-6G basis; it is 3.881 in the 196 CSFs space and is reduced to 3.863 in the 19404 CSFs space with 6-31G basis; and it is 3.894 in the 196 CSFs space reduced to 3.885 in the 5292 CSFs space with 6-31G* basis. The $1\pi_u$ orbital in the linear form of C_2Li_2 well represents the π orbitals between carbons. For the case of the bridged C_2Li_2 , the C—C bond lengths are not affected basically by the change in the occupation numbers in the $4a_g$ and $1b_{3u}$ orbitals. The electron correlation tends to make the C—C bond lengths in the linear C_2Li_2 very close to the counterparts in the planar bridged one; that is especially true with the 6-31G and 6-31G* basis sets. For those active orbitals that correspond to the virtual orbitals in the RHF wave-

Table 39.1. Occupation Numbers For the Active Space in C_2Li_2

($n_a = 7$, 196 CSFs)

Bridged	$3a_g$	$2b_{2u}$	$2b_{1u}$	$4a_g$	$1b_{3u}$	$3b_{1u}$	$5a_g$
STO-6G	2.000	1.998	1.992	1.924	1.924	0.080	0.080
6-31G	2.000	1.997	1.991	1.933	1.933	0.073	0.073
6-31G*	2.000	1.997	1.990	1.937	1.937	0.069	0.069
Linear	$3\sigma_g$	$3\sigma_u$	$4\sigma_g$	$1\pi_u$	$1\pi_u$	$4\sigma_u$	$5\sigma_g$
STO-6G	2.000	1.997	1.986	1.943	1.943	0.068	0.064
6-31G	2.000	1.997	1.985	1.941	1.940	0.070	0.066
6-31G*	2.000	1.996	1.986	1.948	1.946	0.065	0.060

Table 39_2. Occupation Numbers For the Active Space in C_2Li_2

($n_a = 8$, 1176 CSFs)

Bridged	$3a_g$	$2b_{2u}$	$2b_{1u}$	$4a_g$	$1b_{3u}$	$3b_{1u}$	$5a_g$	$1b_{3g}$
STO-6G	1.999	1.991	1.975	1.924	1.924	0.081	0.081	0.026
6-31G	1.999	1.992	1.977	1.935	1.935	0.071	0.071	0.021
6-31G*	1.996	1.991	1.983	1.939	1.939	0.066	0.066	0.018
Linear	$3\sigma_g$	$3\sigma_u$	$4\sigma_g$	$1\pi_u$	$1\pi_u$	$4\sigma_u$	$5\sigma_g$	$1\pi_g$
STO-6G	1.999	1.988	1.963	1.943	1.938	0.068	0.068	0.032
6-31G	1.999	1.988	1.964	1.941	1.940	0.070	0.068	0.031
6-31G*	1.999	1.988	1.967	1.947	1.946	0.064	0.061	0.027

Table 39.3. Occupation Numbers For the Active Space in C_2Li_2

($n_a = 9$, 5292 CSFs)

Bridged	$3a_g$	$2b_{2u}$	$2b_{1u}$	$4a_g$	$1b_{3u}$	$3b_{1u}$	$5a_g$	$1b_{3g}$	$1b_{2g}$
STO-6G	1.991	1.980	1.975	1.921	1.921	0.083	0.083	0.025	0.020
6-31G	1.992	1.980	1.977	1.936	1.936	0.069	0.069	0.020	0.020
6-31G*	1.992	1.981	1.978	1.940	1.940	0.065	0.065	0.019	0.019
Linear	$3\sigma_g$	$3\sigma_u$	$4\sigma_g$	$1\pi_u$	$1\pi_u$	$4\sigma_u$	$5\sigma_g$	$1\pi_g$	$1\pi_g$
STO-6G	1.998	1.982	1.959	1.937	1.935	0.070	0.070	0.039	0.010
6-31G	1.998	1.982	1.961	1.939	1.933	0.070	0.068	0.037	0.011
6-31G*	1.998	1.983	1.964	1.946	1.939	0.065	0.061	0.033	0.011

Table 39.4. Occupation Numbers For the Active Space in C_2Li_2

($n_a = 10$, 19404 CSFs)

Bridged	$3a_g$	$2b_{2u}$	$2b_{1u}$	$4a_g$	$1b_{3u}$	$3b_{1u}$	$5a_g$	$1b_{3g}$	$1b_{2g}$	$2b_{3u}$
STO-6G	1.988	1.976	1.972	1.919	1.912	0.085	0.082	0.031	0.021	0.013
6-31G										
6-31G*	1.990	1.977	1.976	1.939	1.931	0.066	0.065	0.023	0.020	0.013
Linear	$3\sigma_g$	$3\sigma_u$	$4\sigma_g$	$1\pi_u$	$1\pi_u$	$4\sigma_u$	$5\sigma_g$	$1\pi_g$	$1\pi_g$	$2\pi_u$
STO-6G	1.988	1.981	1.957	1.934	1.933	0.072	0.070	0.039	0.011	0.005
6-31G	1.989	1.977	1.975	1.935	1.928	0.070	0.069	0.025	0.020	0.011
6-31G*	1.995	1.980	1.980	1.946	1.945	0.064	0.058	0.018	0.008	0.006

functions, the sum of their occupation numbers increases with the increase in the size of the active space. The electrons in these “virtual” orbitals also influence the energy of the MCSCF wavefunctions, although not in a large and consistent manner. Table 40 shows their occupation numbers along with the relative energy in the MCSCF/6-31G* wavefunctions. Except for the 19404 CSFs space of the linear C_2Li_2 the sum of the “virtual” occupation numbers increases with the size of the active space, so does the MCSCF optimized energy difference between the linear and the bridged forms. For the linear C_2Li_2 in the 19404 CSFs space, the sum of the “virtual” occupation numbers was reduced below the corresponding sum in the 5292 CSFs space. This reduction may contribute to an almost zero value of the MCSCF energy difference.

Table 41 presents the weights of the first three most important configurations in the MCSCF-CASSCF wavefunctions for the linear and bridged C_2Li_2 . Here the weight is given as $\sum C_i^2$, where the C_i^2 are the coefficients of configuration functions in a MCSCF wavefunction, and the sum is over all CSFs. All of the C_i s for the three configurations are shown in Table 8. These three CSFs correspond to the ground state configurations as follows (the active space only):

- Linear C_2Li_2 : $(1\sigma_g)^2 (1\sigma_u)^2 (2\sigma_g)^2 (2\sigma_u)^2 (3\sigma_g)^2 (3\sigma_u)^2$
 $(4\sigma_g)^2 (1\pi_u)^4$
- Bridged C_2Li_2 : $(1a_g)^2 (2b_{2u})^2 (2a_g)^2 (1b_{1u})^2 (3a_g)^2 (2b_{2u})^2$
 $(2b_{1u})^2 (4a_g)^2 (1b_{3u})^2$

Table 40. "Virtual" Occupation Numbers in the
 MCSCF/6-31G* Wavefunction For C₂Li₂

Numbers of CSFs	Sum of the Occ. Num.		$\Delta E^{\dagger}_{\text{Linear-Bridged}}$ kcal/mol
	Linear	Bridged	
196	0.125	0.138	4.9
1176	0.152	0.160	-2.1
5292	0.170	0.168	-7.3
19404	0.154	0.187	-0.4

Table 41. Weights of The First Three Most Important CSFs
in the MCSCF Wavefunctions For C_2Li_2

Basis	Number of Configurations	Linear			Planar Bridged		
		First	Second	Third	First	Second	Third
STO-6G	66	94.1	2.0	1.4	94.1	1.4	1.4
	196	92.2	2.3	1.7	94.1	1.4	1.2
	1176	88.4	2.3	2.0	86.5	6.3	1.4
	5292	86.5	3.2	1.7	84.6	6.8	1.4
	19404	82.8	4.8	2.3	84.6	6.8	1.2
6-31G	66	94.1	1.7	1.2			
	196	92.2	2.0	1.4	94.1	1.7	1.4
	1176	86.5	7.3	1.4	81.0	14.4	1.2
	5292	84.6	5.8	1.2	77.4	13.0	1.2
	19404	90.1	1.4	1.4			
6-31G*	66	94.1	1.4	1.2	94.1	1.4	1.2
	196	94.1	1.7	1.4	94.1	1.4	1.4
	1176	84.6	7.3	1.4	90.3	3.2	1.2
	5292	86.5	4.8	1.2	86.5	5.3	1.2
	19404	90.3	1.4	1.2	92.2	1.4	1.0

† using the optimised geometry in 5292 CSF space

These are the dominant configurations in all MCSCF wavefunctions for C_2Li_2 but their weights are generally reduced with the increase in the number of CSFs, and so are the sum of the weights of these three most important configurations except for the MCSCF(19404 CSFs)/6-31G wavefunction. When the active subspace changes from 5292 CSFs to 19404 CSFs, the total weights of these configurations in that wavefunction are increased (instead of decreased). In particular, the weight of the first one, the ground state configuration, is increased by almost 5 percent while the weight of the second one is decreased by about the same amount. This implies a decrease of an electron correlation effect in the MCSCF/6-31G wavefunction, and might contribute to the observation that the MCSCF relative energy decreases sharply from 18.5 kcal/mol at the 5292 CSF subspace to almost zero at the 19404 CSF subspace. A similar change can be found in the MCSCF(19404 CSFs)/6-31G* wavefunction (see Table 40). It is not clear why increasing the size of the active space actually leads to less, not more, energy difference.

RHF/6-31G* and MCSCF(1176 CSF's)/6-31G* calculations without geometry optimizations were also carried out on several distorted planar bridged C_2Li_2 molecules, in which the angle of Li—C—C is changed and the C—C bond is no longer kept perpendicular to the Li—Li "bond". Figure 2 shows an energy pathway between the linear $D_{\infty h}$ and the planar bridged D_{2h} forms. One can see from this figure that there is a quite flat energy pathway. Although the energies for

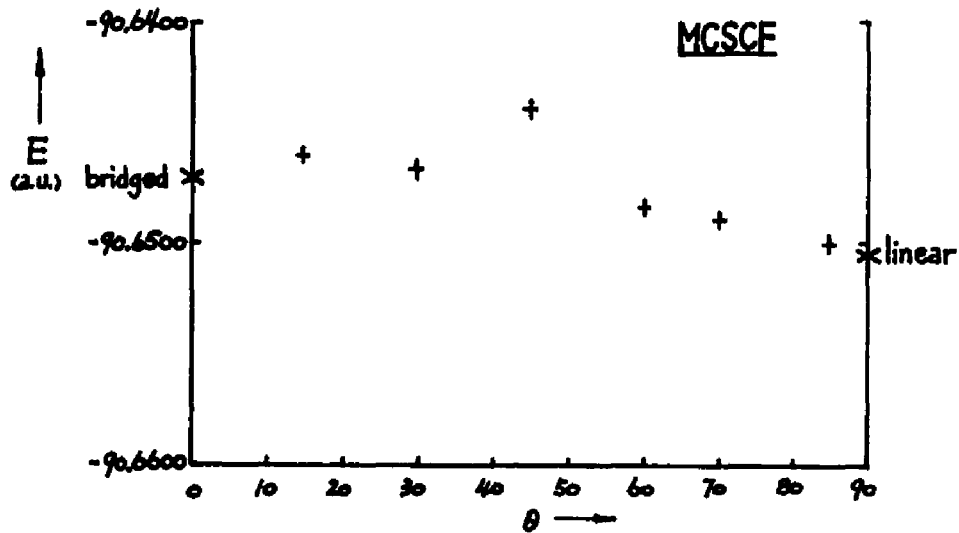
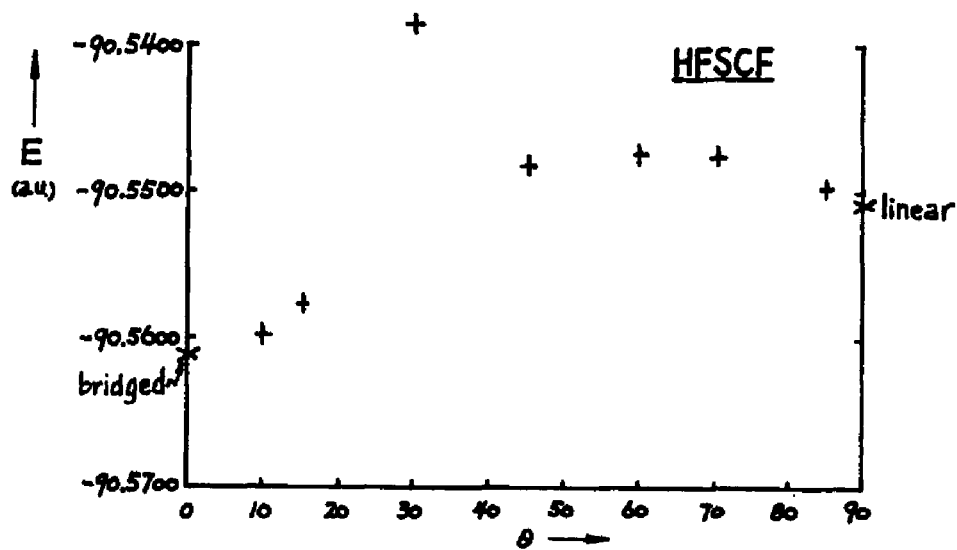
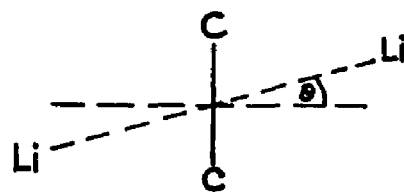


Figure 2. Dependence of Energies of C_2Li_2 on Angle θ

these distorted forms were not obtained from optimized structures, it is not expected this will alter the qualitative description of the C_2Li_2 energy surface.

4.2 Dilithiomethane

4.2.1 Hartree-Fock Structures

The Hartree-Fock optimized energy differences shown in Table 18 indicate that the tetrahedral C_{2v} structures appear to be energy-favorable in both the singlet and triplet states. As illustrated in Table 19 the dilithiomethane molecule is predicted to have a triplet ground state at all but STO-6G minimal basis set.

The C—Li bond lengths in CH_2Li_2 decrease in going from the tetrahedral (1.97 – 1.98 Å) to the trans planar (1.93 – 1.95 Å) to the cis planar (1.83 – 1.85 Å). For the tetrahedral and cis planar forms of the CH_2Li_2 molecule, the drastic change in structure occurs in the Li—C—Li and H—C—Li bond angles, especially the Li—C—Li angles between the singlet and triplet states. The difference for the latter is more than 40 degrees. Due to the spatial arrangement of the cis planar form of CH_2Li_2 (see Figure 3), the cis planar isomer might have a “homoaromatic” bonding in the sense that a three-center (Li, C,

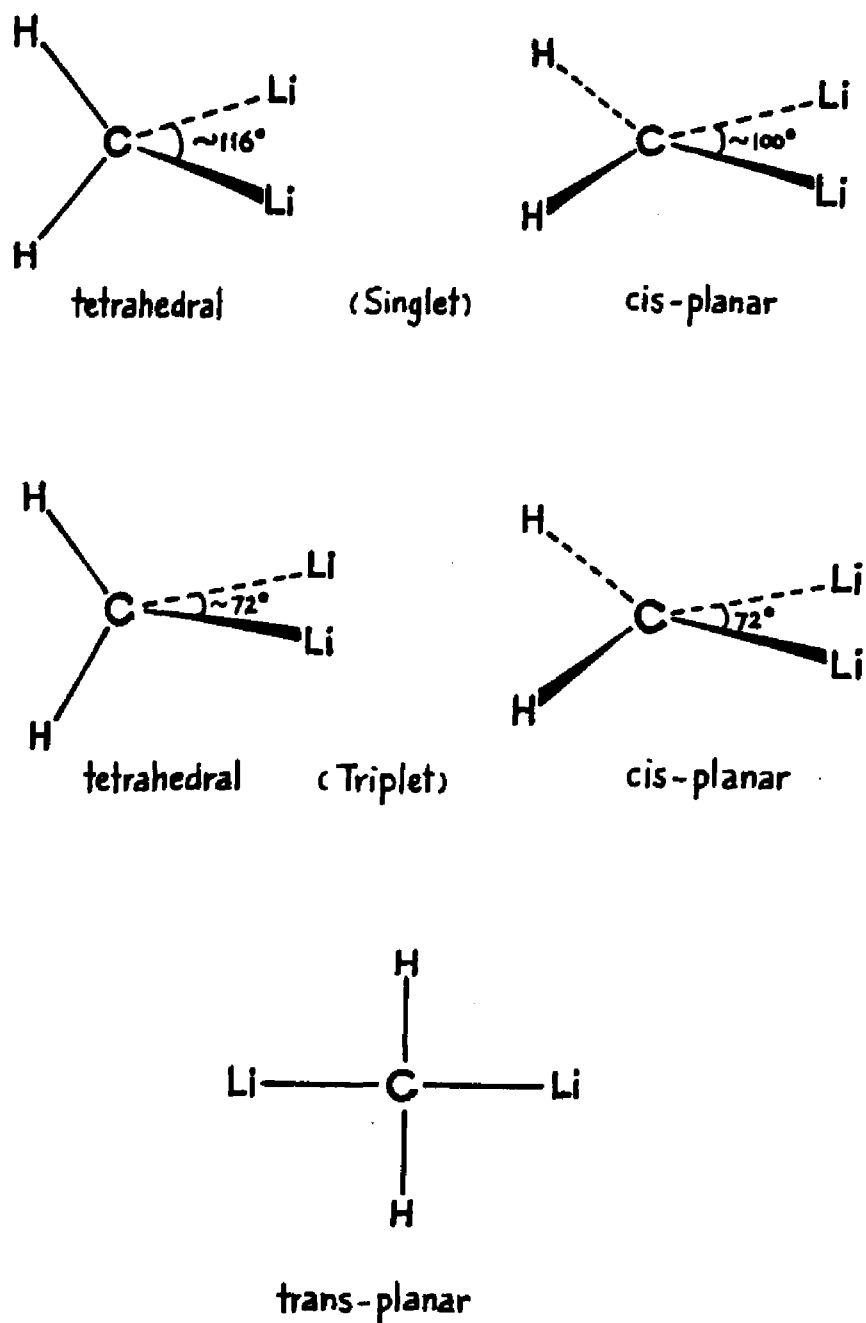


Figure 3. Optimized Geometries For CH_2Li_2

and Li) π bond exists among the two lithium atoms and the central carbon. This is revealed by the Li—Li and C—Li Mulliken overlap populations shown in Tables 27 and 28. For both triplets an electron is removed from a Li—C—Li orbital of π type (symmetry b_1) and placed in a Li—Li σ bonding orbital (symmetry a_1). This results in quite a reduction of the Li—C—Li angle in both triplets and singlet forms, and three-membered rings are formed. The C—Li bond lengthenings reflect the removal of an electron from the π bonding orbital.

4.2.2 MCSCF Structures

One thing is quite clear in terms of the MCSCF energy (see Table 30): since the tetrahedral-like C_{2v} always has the lowest energy for both the singlet and triplet states, therefore the structure of the ground state for dilithiomethane molecule must be in the tetrahedral C_{2v} geometry. The question remains: what is the multiplicity of the ground state for CH_2Li_2 , singlet or triplet? The energy differences are either very small or not quite consistent in the way they vary. The MCSCF energy for the singlet state is lower with the Dunning-Hay (D95V) basis set but higher with both 6-31G* and 6-31G** basis sets.

Table 42 presents the occupation numbers for the active orbitals in all three forms of dilithiomethane molecules. One can see a similar change described previously in the Hartree-Fock structures. The first

Table 42.1. Occupation Numbers For the Active Space in CH₂Li₂

Part. 1 (Singlet $n_a = 8$, 1764 CSFs)

Basis		3a ₁	1b ₁	4a ₁	2b ₂	5a ₁	3b ₂	6a ₁	2b ₁
Tetra	D95V	1.978	1.972	1.951	1.945	0.055	0.048	0.026	0.025
	6-31G*	1.979	1.974	1.955	1.950	0.050	0.044	0.024	0.024
	6-31G**	1.979	1.974	1.955	1.950	0.049	0.044	0.025	0.024
Cis	D95V	1.978	1.972	1.954	1.937	0.062	0.047	0.027	0.025
	6-31G*	1.979	1.974	1.959	1.941	0.059	0.040	0.025	0.024
	6-31G**	1.979	1.974	1.959	1.942	0.058	0.040	0.025	0.024
Basis		3a _g	1b _{2u}	2b _{1u}	1b _{3u}	4a _g	3b _{1u}	2b _{2u}	1b _{3g}
Trans	D95V	1.999	1.982	1.976	1.962	0.035	0.026	0.018	0.002
	6-31G*	1.999	1.983	1.975	1.965	0.031	0.026	0.017	0.005
	6-31G**	1.999	1.983	1.975	1.965	0.030	0.026	0.017	0.005

Table 42.2. Occupation Numbers For the Active Space in CH₂Li₂

Part. 2 (Triplet $n_a = 8$, 7650 CSFs)

Basis		3a ₁	1b ₁	4a ₁	2b ₂	5a ₁	3b ₂	2b ₁	6a ₁	1a ₂
Tetra	D95V	1.978	1.972	1.970	1.001	0.990	0.027	0.027	0.023	0.012
	6-31G*	1.980	1.974	1.973	1.001	0.991	0.024	0.024	0.021	0.011
	6-31G**	1.980	1.974	1.973	1.001	0.991	0.024	0.024	0.021	0.011
Cis	D95V	1.978	1.972	1.970	1.001	0.990	0.028	0.026	0.023	0.013
	6-31G*	1.980	1.975	1.974	1.001	0.991	0.024	0.024	0.021	0.011
	6-31G**	1.980	1.975	1.974	1.001	0.991	0.024	0.024	0.021	0.011
Basis		3a _g	1b _{2u}	2b _{1u}	1b _{3u}	4a _g	3b _{1u}	2b _{2u}	1b _{3g}	1b _{2g}
Trans	D95V	1.977	1.972	1.960	1.000	1.000	0.039	0.031	0.018	0.003
	6-31G*	1.978	1.973	1.964	1.000	1.000	0.033	0.030	0.018	0.004
	6-31G**	1.979	1.973	1.965	1.000	1.000	0.033	0.030	0.017	0.005

most important configurations are:

- Singlet: $(3a_1)^2 (1b_1)^2 (4a_1)^2 (2b_2)^2$
- Triplet: $(3a_1)^2 (1b_1)^2 (4a_1)^2 (2b_2)^1 (5a_1)^1$

The weights of the first three most important configurations included in Table 43 show that there exist many low-lying triplet configurations in the MCSCF wavefunctions, particularly in the MCSCF wavefunctions of the tetrahedral and cis planar CH_2Li_2 . This causes a lowering in energy for the triplet states.

For both the C_2Li_2 and CH_2Li_2 molecules, the presence of Li $2p$ atomic orbitals in the MO's may lead to many excited configurations which have relatively small energies (relative to the ground state). This will have two effects:

1. Such low-lying configurations will make a strong energy contribution to a CI or MCSCF wavefunction
2. Geometries may not be predicted reliably at the RHF level.

A similar behavior also was found in a related alkali-substituted acetylene, viz., for C_2Na_2 molecule, the RHF/STO-6G energy favors the planar bridged form over the linear form by about 20 kcal/mol.

Table 43. Weights of First Three Most Important CSFs
in the MCSCF Wavefunction For CH₂Li₂

Basis		Singlet			Triplet		
		First	Second	Third	First	Second	Third
Tetra	D95V	92.2	1.2	1.0	29.2	29.2	17.6
	6-31G*	92.2	1.2	1.0	30.3	27.0	20.3
	6-31G**	92.2	1.2	1.0	30.3	27.0	18.5
Cis	D95V	92.2	0.5	0.5	60.8	33.6	0.3
	6-31G*	92.2	1.7	0.6	57.8	37.2	0.2
	6-31G**	92.2	1.4	0.6	54.8	41.0	0.2
Trans	D95V	96.0	0.1	0.05	82.8	8.4	1.2
	6-31G*	96.0	0.1	0.05	94.1	0.05	0.05
	6-31G**	96.0	0.1	0.05	96.0	0.08	0.04

Chapter 5

Conclusions

5.1 Dilithioacetylene

Which structure, linear or planar bridged, is “correct”? Theoretical optimized structures refer to isolated species; the most suitable experimental data involve measurements in dilute gas. In the absence of experimental gas phase structural data on the dilithioacetylene monomer, this question is hard to answer definitely. Calculations reported in this study reveal a large dependence of optimized geometries and energies on the basis set at the single determinant Hartree-Fock level of theory. The linear structure is favored over the planar bridged form in larger active multiconfiguration spaces at the MCSCF level. It seems reasonable to conclude

1. The dilithioacetylene molecule, C_2Li_2 , has a rather flat potential energy surface;
2. The calculations do not conclusively favor either the linear or planar bridged forms

3. However, at the MCSCF level with 6-31G* basis, larger active configuration spaces appear to favor the linear $D_{\infty h}$ form.

Not long ago, Jaworski et al. published a study of C_2Li_2 [33]. They carried out the Hartree-Fock (RHF) theory, Many-Body perturbation theory (MBPT) and Coupled Cluster theory (CCT) calculations with 6-31G*, 6-311G* (contains five d functions), 6-311G* (without sp shell on Li) and regular 6-311G* (i.e., six d functions) basis sets. Geometry optimizations were carried out at the HF level for both D_{2h} and $D_{\infty h}$ and at the MBPT level for D_{2h} and C_{2v} (a bent doubly-bridged form) but not $D_{\infty h}$. Then higher-order energy corrections to the MBPT second-order energies with the regular 6-311G* basis were performed only on the D_{2h} and C_{2v} . Their HF relative energies with 6-31G* and the regular 6-311G* bases are almost identical to those reported in this work, which are about 6 – 7 kcal/mol and the bridged form is lower in energy. Their MBPT(2)/6-31G*, i.e., MP2/6-31G*, calculation found that the C_{2v} form is lower in energy, which is in contrast with that calculated in the present work. Their higher-order corrections still favor the D_{2h} . Based on the above, they claimed that the planar bridged D_{2h} structure is the configuration with absolute minimum in energy. Several remarks are made on their work as follows:

1. Their HF SCF results are very close to those from this work,
2. It is very hard to judge their MBPT results because

- there is no MBPT energy for the $D_{\infty h}$ form provided in their work¹
 - they did not explain why the $D_{\infty h}$ form was not included in their MBPT treatment
3. Comparing their MBPT(2) and higher-order corrections against the MP2, MP3, MP4SDQ, and MP4SDTQ results reported in this work, both reach the same conclusion, that is, D_{2h} is the minimum in energy.
 4. Due to the nature of the MBPT and CCSD methods used by them and the fact that not enough data were provided, their conclusion is not convincing and still open to controversy.

MBPT as well as CCSD methods are not variational and the total electronic energy obtained using them can be lower than the true energy since they tend to overestimate the correlation energy, in certain cases, as much as 120 %. Therefore, a conclusion drawn solely from MBPT or MBPT-like energy is debatable.

5.2 Dilithiomethane

All Hartree-Fock (RHF, ROHF, UHF) and MCSCF calculations show that the tetrahedral-like C_{2v} form always is the lowest in energy among

¹Though Disch et al. show [78] that second-order correlation corrections to the 6-31G*(SCF) calculations favors the D_{2h} form by 9.6 kcal/mol.

the three symmetries of tetrahedral C_{2v} , cis planar C_{2v} and trans planar D_{2h} for both the singlet and triplet states, so does the CISD/6-31G* calculations for the singlet state of the CH_2Li_2 molecule. Therefore it is reasonably certain that the dilithiomethane molecule has a tetrahedral-like C_{2v} ground state geometry. However, since this molecule does not show very strong preferences for the tetrahedral-like structure (the energy difference between the tetrahedral and cis planar forms is very small, only a few kilocalories per mole), a question still remains: if the cis planar is not the ground state structure, then what could it be: a transition state?

A conclusive answer to the question of the ground electronic state is not possible, but it appears that the ground electronic state is not the trans planar D_{2h} . For the cis planar form of CH_2Li_2 , the triplet state is not much more stable than the singlet state. For the tetrahedral-like C_{2v} form, it is difficult to assign the ground state configuration of CH_2Li_2 even at the MCSCF CASSCF level of theory. The singlet and the triplet states are almost indistinguishable in energy.

At this point many basic questions concerning the ground state geometries and electronic states of dilithioacetylene and dilithiomethane remain unresolved. For instance, what is there about the lithium atom(s) which leads to such unusual geometries in the molecules in which it occurs? Furthermore, final resolution of the questions will almost certainly require the use of huge amounts of computer time, even if state-of-the-art supercomputers are used. The problem also

remains: given the required computer time, just what theoretical approach is most likely to provide definitive solutions to the puzzles posed by lithiated hydrocarbon molecules?

APPENDIXES

The Orbital Symmetry Assignment For Planar Bridged C_2Li_2

Basis	Occupied	Virtual
STO-6G	$(A_g)(B_{2u})(B_{1u})(A_g)$ $(A_g)(B_{2u})(B_{1u})(A_g)$ (B_{3u})	$(B_{1u})(A_g)(B_{3g})(B_{2g})(B_{3u})(B_{2u})$ $(A_g)(B_{1g})(B_{3g})(B_{1u})(B_{2u})$
6-31G	$(A_g)(B_{2u})(A_g)(B_{1u})$ $(A_g)(B_{2u})(B_{1u})(A_g)$ (B_{3u})	$(B_{1u})(A_g)(B_{3g})(B_{2g})(B_{3u})(B_{2u})$ $(B_{1u})(A_g)(B_{3g})(A_g)(B_{2g})(B_{1u})$ $(B_{3u})(B_{2u})(B_{1g})(B_{3g})(A_g)(B_{1u})$ $(B_{2u})(A_g)(B_{3u})(B_{1g})(B_{3g})(B_{2u})$ $(A_g)(B_{1u})(B_{2u})$
6-31G*	$(A_g)(B_{2u})(A_g)(B_{1u})$ $(A_g)(B_{2u})(B_{1u})(A_g)$ (B_{3u})	$(B_{1u})(A_g)(B_{3g})(B_{2g})(B_{3u})(B_{2u})$ $(B_{1u})(A_g)(B_{3g})(A_g)(B_{2g})(B_{1u})$ $(B_{3u})(B_{2u})(B_{1g})(B_{3g})(A_g)(B_{1u})$ $(A_u)(B_{1u})(B_{2g})(A_g)(B_{2u})(B_{1g})$ $(B_{3u})(B_{2u})(A_g)(B_{3g})(A_g)(B_{3u})$ $(B_{1g})(B_{1u})(A_g)(B_{2u})(B_{3g})(B_{1u})$ $(A_g)(B_{2u})(B_{1u})(B_{3u})(B_{1u})(B_{2g})$ $(A_g)(A_u)(B_{2u})(A_g)(B_{1g})(B_{3g})$ $(B_{2u})(B_{2u})(A_g)$

The Orbital Symmetry Assignment For Linear C₂Li₂

Basis	Occupied	Virtual
STO-6G	$(\sigma_g)(\sigma_u)(\sigma_u)(\sigma_g)$ $(\sigma_g)(\sigma_u)(\sigma_g)(\pi_u)$ (π_u)	$(\sigma_u)(\sigma_g)(\pi_g)(\pi_g)(\pi_u)(\pi_u)$ $(\sigma_u)(\sigma_g)(\pi_g)(\pi_g)(\sigma_u)$
6-31G	$(\sigma_g)(\sigma_u)(\sigma_u)(\sigma_u)$ $(\sigma_g)(\sigma_u)(\sigma_g)(\pi_u)$ (π_u)	$(\sigma_u)(\sigma_g)(\pi_g)(\pi_g)(\pi_u)(\pi_u)$ $(\sigma_u)(\sigma_g)(\sigma_g)(\pi_g)(\pi_g)(\sigma_u)$ $(\pi_u)(\pi_u)(\pi_g)(\pi_g)(\sigma_g)(\sigma_u)$ $(\sigma_u)(\pi_u)(\pi_u)(\sigma_g)(\pi_g)(\pi_g)$ $(\sigma_g)(\sigma_u)(\sigma_u)$
6-31G*	$(\sigma_g)(\sigma_u)(\sigma_u)(\sigma_u)$ $(\sigma_g)(\sigma_u)(\sigma_g)(\pi_u)$ (π_u)	$(\sigma_u)(\sigma_g)(\pi_g)(\pi_g)(\pi_u)(\pi_u)$ $(\sigma_u)(\sigma_g)(\sigma_g)(\pi_g)(\pi_g)(\sigma_u)$ $(\pi_u)(\pi_u)(\pi_g)(\pi_g)(\sigma_g)(\sigma_u)$ $(\Delta_g)(\Delta_g)(\Delta_u)(\Delta_u)(\pi_u)(\pi_u)$ $(\pi_g)(\pi_g)(\sigma_u)(\sigma_g)(\pi_u)(\pi_u)$ $(\sigma_g)(\sigma_u)(\pi_g)(\pi_g)(\sigma_g)(\sigma_u)$ $(\sigma_g)(\sigma_u)(\sigma_u)(\Delta_g)(\Delta_g)(\pi_u)$ $(\pi_u)(\Delta_u)(\Delta_u)(\sigma_g)(\pi_g)(\pi_g)$ $(\sigma_u)(\sigma_g)(\sigma_u)$

The Orbital Symmetry Assignment For Tetra CH₂Li₂ (Singlet)

Basis	Occupied	Virtual
D95V	(A ₁)(A ₁)(B ₂)(A ₁)(B ₁) (A ₁)(B ₂)	(A ₁)(B ₂)(A ₁)(B ₁)(A ₂)(B ₂)(A ₁) (B ₂)(A ₁) (A ₁)(B ₁)(A ₂)(B ₂)(B ₂)(A ₁)(A ₁) (B ₁)(B ₂) (B ₁)(A ₁)(B ₂)(B ₂)(A ₁)(A ₁)(B ₁)
	The Electronic State is ¹ A ₁ .	
6-31G*	(A ₁)(A ₁)(B ₂)(A ₁)(B ₁) (A ₁)(B ₂)	(A ₁)(B ₂)(A ₁)(B ₁)(A ₂)(B ₂)(A ₁) (B ₂)(A ₁) (A ₁)(B ₁)(B ₂)(A ₂)(B ₂)(A ₁)(B ₁) (A ₁)(B ₂) (A ₁)(B ₁)(A ₂)(A ₁)(B ₂)(B ₁)(A ₂) (B ₂)(A ₁) (B ₂)(A ₁)(B ₂)(A ₁)(B ₁)(B ₁)(A ₁) (B ₂)(A ₁) (A ₂)(A ₁)(B ₂)(A ₁)(B ₁)(A ₁)
	The Electronic State is ¹ A ₁ .	
6-31G**	(A ₁)(A ₁)(B ₂)(A ₁)(B ₁) (A ₁)(B ₂)	(A ₁)(B ₂)(A ₁)(B ₁)(A ₂)(B ₂)(A ₁) (B ₂)(A ₁) (A ₁)(B ₁)(B ₂)(A ₂)(B ₂)(A ₁)(B ₁) (A ₁)(B ₂) (A ₁)(B ₁)(A ₂)(A ₁)(B ₂)(B ₁)(A ₂) (B ₂)(A ₁) (B ₂)(A ₁)(B ₂)(B ₁)(A ₁)(B ₁)(A ₁) (B ₂)(A ₁) (A ₂)(A ₁)(B ₂)(A ₁)(B ₁)(B ₁)(B ₂) (A ₂)(A ₁) (A ₁)(B ₁)(A ₁)
	The Electronic State is ¹ A ₁ .	

The Orbital Symmetries For Cis CH₂Li₂ (Singlet)

Basis	Occupied	Virtual
DH	(A ₁) (A ₁) (B ₂) (A ₁) (B ₂) (A ₁) (B ₁)	(A ₁) (B ₂) (A ₁) (A ₂) (B ₂) (B ₁) (A ₁) (B ₂) (A ₁) (A ₁) (B ₁) (A ₂) (B ₂) (B ₂) (A ₁) (B ₂) (A ₁) (B ₂) (A ₁) (B ₁) (B ₂) (A ₁) (B ₂) (A ₁)
	The Electronic State is ¹ A ₁ .	
6-31G*	(A ₁) (A ₁) (B ₂) (A ₁) (B ₂) (A ₁) (B ₁)	(A ₁) (B ₂) (A ₁) (A ₂) (B ₂) (B ₁) (A ₁) (B ₂) (A ₁) (A ₁) (B ₂) (B ₁) (A ₂) (B ₂) (A ₁) (B ₂) (A ₁) (B ₁) (B ₂) (A ₁) (A ₂) (A ₁) (B ₂) (B ₁) (A ₂) (B ₂) (A ₁) (B ₁) (B ₂) (A ₁) (A ₁) (A ₁) (B ₂) (B ₂) (A ₁) (B ₂) (A ₂) (A ₁) (B ₁) (A ₁) (B ₂) (A ₁)
	The Electronic State is ¹ A ₁ .	
6-31G**	(A ₁) (A ₁) (B ₂) (A ₁) (B ₂) (A ₁) (B ₁)	(A ₁) (B ₂) (A ₁) (A ₂) (B ₂) (B ₁) (A ₁) (B ₂) (A ₁) (A ₁) (B ₂) (B ₁) (A ₂) (B ₂) (A ₁) (B ₂) (A ₁) (B ₁) (B ₂) (A ₂) (A ₁) (A ₁) (B ₂) (B ₁) (A ₂) (B ₂) (A ₁) (B ₁) (B ₂) (A ₁) (A ₁) (A ₁) (B ₂) (B ₂) (A ₁) (B ₂) (A ₂) (A ₁) (B ₁) (A ₁) (B ₂) (B ₂) (B ₁) (A ₂) (A ₁) (A ₁) (B ₂) (A ₁)
	The Electronic State is ¹ A ₁ .	

The Orbital Symmetry Assignment For Trans CH₂Li₂ (Singlet)

Basis	Occupied	Virtual
DH	(A _g) (B _{1u}) (A _g) (A _g) (B _{2u}) (B _{1u}) (B _{3u})	(A _g) (B _{1u}) (B _{2u}) (B _{3g}) (B _{2g}) (B _{3u}) (A _g) (B _{1u}) (A _g) (B _{3g}) (B _{2g}) (B _{1u}) (B _{2u}) (B _{3u}) (A _g) (A _g) (B _{1u}) (B _{2u}) (B _{2u}) (B _{3u}) (B _{1u}) (A _g) (A _g) (B _{2u})
	The Electronic State is ¹ A _g .	
6-31G*	(A _g) (B _{1u}) (A _g) (A _g) (B _{2u}) (B _{1u}) (B _{3u})	(A _g) (B _{1u}) (B _{2u}) (B _{3g}) (B _{2g}) (B _{3u}) (A _g) (B _{1u}) (A _g) (B _{3g}) (B _{1u}) (B _{2g}) (B _{2u}) (B _{3u}) (A _g) (A _g) (B _{2u}) (B _{1u}) (B _{1g}) (B _{3g}) (B _{1u}) (A _u) (B _{2g}) (A _g) (B _{3u}) (B _{2u}) (A _g) (B _{1u}) (B _{3u}) (A _g) (B _{2u}) (A _g) (B _{1u}) (A _g) (B _{2u}) (B _{1u}) (B _{1g}) (B _{3g}) (B _{2g}) (A _g) (A _g) (A _g)
	The Electronic State is ¹ A _g .	
6-31G**	(A _g) (B _{1u}) (A _g) (A _g) (B _{2u}) (B _{1u}) (B _{3u})	(A _g) (B _{1u}) (B _{2u}) (B _{3g}) (B _{2g}) (B _{3u}) (A _g) (B _{1u}) (A _g) (B _{3g}) (B _{1u}) (B _{2g}) (B _{2u}) (B _{3u}) (A _g) (A _g) (B _{2u}) (B _{1u}) (B _{1g}) (B _{3g}) (B _{1u}) (A _u) (B _{2g}) (A _g) (B _{3u}) (B _{2u}) (A _g) (B _{1u}) (B _{3u}) (A _g) (B _{2u}) (A _g) (B _{1u}) (A _g) (B _{2u}) (B _{1u}) (B _{1g}) (B _{3g}) (B _{2g}) (A _g) (B _{3u}) (B _{1u}) (A _g) (B _{3g}) (B _{1g}) (B _{2u}) (A _g) (A _g)
	The Electronic State is ¹ A _g .	

The Orbital Symmetry Assignment For Tetra CH₃Li₂ (Triplet)

Basis	Occupied	Virtual
	Alpha Orbitals	
	(A ₁)(A ₁)(B ₂)(A ₁)(B ₁)	(B ₂)(B ₁)(A ₁)(A ₂)(B ₂)(A ₁)(B ₂) (A ₁)(B ₁)
	(A ₁)(B ₂)(A ₁)	(A ₁)(A ₂)(B ₂)(B ₂)(A ₁)(A ₁)(B ₁) (B ₂)(B ₁)
		(A ₁)(B ₂)(A ₁)(A ₁)(B ₁)
DH	Beta Orbitals	
	(A ₁)(A ₁)(B ₂)(A ₁)(B ₁)	(B ₂)(A ₁)(B ₁)(A ₁)(B ₂)(A ₂)(A ₁) (B ₂)(B ₂)
	(A ₁)	(B ₁)(A ₁)(A ₁)(A ₂)(B ₂)(B ₂)(A ₁) (A ₁)(B ₁)
		(B ₂)(B ₁)(A ₁)(B ₂)(A ₁)(A ₁)(B ₁)
	The Electronic State is ³ B ₂ .	
	Alpha Orbitals	
	(A ₁)(A ₁)(B ₂)(A ₁)(B ₁)	(B ₂)(B ₁)(A ₁)(A ₂)(B ₂)(A ₁)(B ₂) (A ₁)(B ₁)
	(A ₁)(B ₂)(A ₁)	(A ₁)(B ₂)(A ₂)(B ₂)(A ₁)(A ₁)(B ₁) (B ₂)(A ₁)
		(B ₁)(B ₁)(A ₂)(A ₁)(B ₂)(A ₁)(A ₂) (B ₂)(B ₂)
		(A ₁)(B ₁)(B ₂)(B ₁)(A ₁)(A ₁)(A ₁) (B ₂)(A ₂)
		(A ₁)(B ₂)(A ₁)(B ₁)(A ₁)
6-31G*	Beta Orbitals	
	(A ₁)(A ₁)(B ₂)(A ₁)(B ₁)	(B ₂)(A ₁)(B ₁)(A ₁)(B ₂)(A ₂)(A ₁) (B ₂)(B ₁)
	(A ₁)	(B ₂)(A ₁)(A ₁)(B ₂)(A ₂)(B ₂)(A ₁) (B ₁)(A ₁)
		(B ₂)(B ₁)(A ₁)(B ₁)(A ₂)(A ₁)(B ₂) (A ₁)(A ₂)
		(B ₂)(A ₁)(B ₂)(B ₁)(B ₂)(B ₁)(A ₁) (A ₁)(B ₂)
		(A ₁)(A ₂)(A ₁)(B ₂)(A ₁)(B ₁)(A ₁)
	The Electronic State is ³ B ₂ .	
	Alpha Orbitals	
	(A ₁)(A ₁)(B ₂)(A ₁)(B ₁)	(B ₂)(B ₁)(A ₁)(A ₂)(B ₂)(A ₁)(B ₂) (A ₁)(B ₁)
	(A ₁)(B ₂)(A ₁)	(A ₁)(B ₂)(A ₂)(B ₂)(A ₁)(A ₁)(B ₁) (B ₂)(A ₁)
		(B ₁)(B ₁)(A ₂)(A ₁)(B ₂)(A ₁)(A ₂) (B ₂)(B ₂)
		(A ₁)(B ₁)(B ₂)(B ₁)(A ₁)(A ₁)(A ₁) (B ₂)(A ₂)
		(A ₁)(B ₂)(A ₁)(B ₁)(B ₁)(B ₂)(A ₂) (A ₁)(A ₁)
		(B ₁)(A ₁)
6-31G**	Beta Orbitals	
	(A ₁)(A ₁)(B ₂)(A ₁)(B ₁)	(B ₂)(A ₁)(B ₁)(A ₁)(B ₂)(A ₂)(A ₁) (B ₂)(B ₁)
	(A ₁)	(B ₂)(A ₁)(A ₁)(B ₂)(A ₂)(B ₂)(A ₁) (B ₁)(A ₁)
		(B ₂)(B ₁)(A ₁)(B ₁)(A ₂)(A ₁)(B ₂) (A ₁)(A ₂)
		(B ₂)(A ₁)(B ₂)(B ₁)(B ₂)(B ₁)(A ₁) (A ₁)(A ₁)
		(B ₂)(A ₂)(A ₁)(B ₂)(A ₁)(B ₁)(B ₁) (B ₂)(A ₂)
		(A ₁)(A ₁)(B ₁)(A ₁)
	The Electronic State is ³ B ₂ .	

The Orbital Symmetries For Cis CH₂Li₂ (Triplet)

Basis	Occupied	Virtual
DH	Alpha Orbitals	
	(A ₁)(A ₁)(B ₂)(A ₁)(B ₂)	(B ₂)(A ₁)(B ₁)(A ₂)(B ₂)(A ₁)(B ₂) (A ₁)(B ₁)
	(A ₁)(B ₁)(A ₁)	(A ₁)(A ₂)(B ₂)(B ₂)(A ₁)(B ₂)(A ₁) (B ₁)(B ₂) (A ₁)(B ₂)(A ₁)(A ₁)(B ₂)
DH	Beta Orbitals	
	(A ₁)(A ₁)(B ₂)(A ₁)(B ₂)	(A ₁)(B ₂)(B ₁)(A ₁)(A ₂)(B ₂)(A ₁) (B ₂)(B ₁)
	(A ₁)	(A ₁)(A ₁)(B ₁)(A ₂)(B ₂)(B ₂)(A ₁) (B ₂)(A ₁) (B ₂)(A ₁)(B ₁)(B ₂)(A ₁)(A ₁)(B ₂)
The Electronic State is ³ B ₁ .		
6-31G*	Alpha Orbitals	
	(A ₁)(A ₁)(B ₂)(A ₁)(B ₂)	(B ₂)(A ₁)(B ₁)(A ₂)(B ₂)(A ₁)(B ₂) (A ₁)(B ₁)
	(A ₁)(B ₁)(A ₁)	(A ₁)(B ₂)(A ₂)(B ₂)(A ₁)(B ₂)(A ₁) (B ₁)(A ₁) (B ₂)(B ₁)(A ₂)(A ₁)(B ₂)(A ₂)(B ₂) (B ₁)(A ₁) (A ₁)(B ₂)(B ₂)(A ₁)(A ₁)(B ₂)(A ₁) (B ₂)(A ₂) (B ₁)(A ₁)(A ₁)(B ₂)(A ₁)
6-31G*	Beta Orbitals	
	(A ₁)(A ₁)(B ₂)(A ₁)(B ₂)	(A ₁)(B ₂)(B ₁)(A ₁)(A ₂)(B ₂)(A ₁) (B ₂)(B ₁)
	(A ₁)	(A ₁)(A ₁)(B ₂)(B ₁)(A ₂)(B ₂)(A ₁) (B ₂)(A ₁) (B ₁)(A ₁)(B ₂)(A ₂)(B ₁)(A ₁)(B ₂) (A ₂)(B ₂) (A ₁)(B ₁)(A ₁)(B ₂)(B ₂)(A ₁)(A ₁) (B ₂)(A ₁) (B ₂)(A ₂)(B ₁)(A ₁)(A ₁)(B ₂)(A ₁)
The Electronic State is ³ B ₁ .		
6-31G**	Alpha Orbitals	
	(A ₁)(A ₁)(B ₂)(A ₁)(B ₂)	(B ₂)(A ₁)(B ₁)(A ₂)(B ₂)(A ₁)(B ₂) (A ₁)(B ₁)
	(A ₁)(B ₁)(A ₁)	(A ₁)(B ₂)(A ₂)(B ₂)(A ₁)(B ₂)(A ₁) (B ₁)(A ₁) (B ₂)(B ₁)(A ₂)(A ₁)(B ₂)(A ₂)(B ₂) (B ₁)(A ₁) (A ₁)(B ₂)(A ₁)(B ₂)(A ₁)(B ₂)(A ₁) (B ₂)(A ₂) (B ₁)(A ₁)(A ₁)(B ₂)(B ₂)(B ₁)(A ₂) (A ₁)(A ₁) (B ₂)(A ₁)
6-31G**	Beta Orbitals	
	(A ₁)(A ₁)(B ₂)(A ₁)(B ₂)	(A ₁)(B ₂)(B ₁)(A ₁)(A ₂)(B ₂)(A ₁) (B ₂)(B ₁)
	(A ₁)	(A ₁)(A ₁)(B ₂)(B ₁)(A ₂)(B ₂)(A ₁) (B ₂)(A ₁) (B ₁)(A ₁)(B ₂)(A ₂)(B ₁)(A ₁)(B ₂) (A ₂)(B ₂) (A ₁)(B ₁)(A ₁)(B ₂)(A ₁)(B ₂)(A ₁) (B ₂)(A ₁) (B ₂)(A ₂)(A ₁)(B ₁)(A ₁)(B ₂)(B ₂) (B ₁)(A ₂) (A ₁)(A ₁)(B ₂)(A ₁)
The Electronic State is ³ B ₁ .		

The Orbital Symmetry Assignment For Trans CH₂Li₂ (Triplet)

Basis	Occupied	Virtual
	Alpha Orbitals (A _g)(B _{1u})(A _g)(A _g)(B _{2u}) (B _{3u})(B _{1u})(A _g)	(B _{1u})(B _{2u})(B _{3u})(B _{3g})(B _{2g})(A _g)(B _{1u}) (A _g)(B _{3g})(B _{2g})(B _{2u})(B _{1u})(B _{3u})(A _g) (A _g)(B _{1u})(B _{2u})(B _{3u})(B _{2u})(B _{1u})(A _g) (A _g)(B _{2u})
DH	Beta Orbitals (A _g)(B _{1u})(A _g)(A _g) (B _{2u})(B _{1u})	(A _g)(B _{1u})(B _{3u})(B _{2u})(B _{3g})(B _{2g})(A _g) (B _{1u})(B _{3u})(A _g)(B _{3g})(B _{2g})(B _{2u})(B _{1u}) (B _{3u})(A _g)(A _g)(B _{1u})(B _{2u})(B _{2u})(B _{3u}) (B _{1u})(A _g)(A _g)(B _{2u})
The Electronic State is ³ B _{3u} .		
	Alpha Orbitals (A _g)(B _{1u})(A _g)(A _g) (B _{2u})(B _{1u})(B _{3u})(A _g)	(B _{1u})(B _{2u})(B _{3g})(B _{2g})(B _{3u})(A _g)(B _{1u}) (A _g)(B _{3g})(B _{2u})(B _{2g})(B _{1u})(B _{3u})(A _g) (A _g)(B _{2u})(B _{1u})(B _{3g})(B _{1g})(B _{2g})(B _{1u}) (A _u)(A _g)(B _{3u})(B _{2u})(A _g)(B _{1u})(B _{3u}) (A _g)(B _{2u})(A _g)(B _{1u})(A _g)(B _{2u})(B _{1u}) (B _{1g})(B _{3g})(B _{2g})(A _g)(A _g)(A _g)
6-31G*	Beta Orbitals (A _g)(A _g)(B _{1u})(A _g) (B _{2u})(B _{3u})	(B _{1u})(A _g)(B _{2u})(B _{3g})(B _{1u})(B _{2g})(B _{3u}) (A _g)(B _{1u})(A _g)(B _{3g})(B _{2u})(B _{2g})(B _{3u}) (B _{1u})(A _g)(A _g)(B _{2u})(B _{1u})(B _{3g})(B _{1g}) (B _{1u})(A _u)(B _{2g})(A _g)(B _{3u})(B _{2u})(A _g) (B _{1u})(B _{3u})(A _g)(B _{2u})(A _g)(B _{1u})(A _g) (B _{2u})(B _{1u})(B _{1g})(B _{3g})(B _{2g})(A _g)(A _g) (A _g)
The Electronic State is ³ B _{3u} .		
	Alpha Orbitals (A _g)(B _{1u})(A _g)(A _g) (B _{2u})(B _{1u})(B _{3u})(A _g)	(B _{1u})(B _{2u})(B _{3g})(B _{2g})(B _{3u})(A _g)(B _{1u}) (A _g)(B _{3g})(B _{2u})(B _{2g})(B _{1u})(B _{3u})(A _g) (A _g)(B _{2u})(B _{1u})(B _{3g})(B _{1g})(B _{2g})(B _{1u}) (A _u)(A _g)(B _{3u})(B _{2u})(A _g)(B _{1u})(B _{3u}) (B _{2u})(A _g)(A _g)(B _{1u})(A _g)(B _{2u})(B _{1u}) (B _{1g})(B _{3g})(B _{2g})(A _g)(B _{3u})(B _{1u})(A _g) (B _{3g})(B _{1g})(B _{2u})(A _g)(A _g)
6-31G**	Beta Orbitals (A _g)(A _g)(B _{1u})(A _g) (B _{2u})(B _{3u})	(B _{1u})(A _g)(B _{2u})(B _{3g})(B _{1u})(B _{2g})(B _{3u}) (A _g)(B _{1u})(A _g)(B _{3g})(B _{2u})(B _{2g})(B _{3u}) (B _{1u})(A _g)(A _g)(B _{2u})(B _{1u})(B _{3g})(B _{1g}) (B _{1u})(A _u)(B _{2g})(A _g)(B _{3u})(B _{2u})(A _g) (B _{1u})(B _{3u})(A _g)(B _{2u})(A _g)(B _{1u})(A _g) (B _{2u})(B _{1u})(B _{1g})(B _{3g})(B _{2g})(A _g)(B _{3u}) (B _{1u})(A _g)(B _{3g})(B _{1g})(B _{2u})(A _g)(A _g)
The Electronic State is ³ B _{3u} .		

LIST OF REFERENCES

1. Clark, T., Schleyer, P.v.R., Houk, K.N. and Rondan, N.G., *J. Chem. Soc., Chem. Commun.* No.12, 579(1981). Rondan, N.G., Houk, K.N., Beak, P., Zajdel, W.J., Chandrasekhar, J. and Schleyer, P.v.R., *J. Org. Chem.* 46, 4108(1981).
2. Wakefield, B.J., *The Chemistry of Organolithium Compounds*, Pergamon Press, New York, 1974.
3. Binkley, J.S., Whiteside, R.A., Krishnan, R., Seeger, R., Schlegel, H.B., Defrees, D.J., Topiol, S. and Pople, J.A., *GAUSSIAN80, QCPE*, 13, 406(1981).
4. Binkley, J.S., Frisch, M.J., Defrees, D.J., Raghavachare, K., Whiteside, R.A., Schlegel, H.B., Fluder, E.M. and Pople, J.A., *GAUSSIAN82*, Department of Chemistry, Carnegie-Mellon University, Pittsburgh, PA.
5. Duplis, M., Spangler, D. and Wendoloski, J.J., *NRCC Software Catalog*, University of California, Berkeley, CA(1980). Schmidt, M.W., Boatz, J.A., Baldrige, K.K., Koseki, S., Gordon, M.S., Elbert, S.T. and Lam, B., *QCPE Bulletin*, Vol.7, 115(1987).
6. Collins, J.B., Dill, J.D., Jemmis, E.D., Apeloig, Y., Schleyer, P.v.R., Seeger, R. and Pople, J.A., *J. Am. Chem. Soc.* **98** 5419(1976).
7. Chandrasekhar, J. and Schleyer, P.v.R., *J. Chem. Soc., Chem. Commun.* no.6 260(1981)
8. Apeloig, Y., Schleyer, P.v.R., Binkley, J.S. and Pople, J.A., *J. Am. Chem. Soc.* **98**, 4332(1976).
9. Laidig, W.D. and Schaefer III, H.F., *ibid.*, 101, 7184(1979).
10. Apeloig, Y. Schleyer, P.v.R. Binkley, J.S., Pople, J.A. and Jorgensen, W.L., *TetrahedronLett.*, 3923(1976).
11. Clark, T. and Schleyer, P.v.R., *J. Chem. Soc., Chem. Commun.* No.20, 883(1979).
12. Vincent, M.A. and Schaefer III, H.F., *J. Chem. Phys.* **77**, 6103(1982).
13. Schleyer, P.v.R., Clark, T., Kos, A.J., Spitznagel, G.W., Rohde, C., Arad, D., Houk, K.N. and Rondan, *J. Am. Chem. Soc.* **106**, 6467(1983).
14. Apeloig, Y., Clark, T., Kos, A.J., Jemmis, E.D. and Schleyer, P.v.R., *Israel J. Chem.* **20**, 43(1980).

15. Schleyer, P.v.R. and Kos, A.J., *J. Chem. Soc., Chem. Commun.* No.12, 448(1982).
16. Schriver, G.W., Klein, J., Kost, D. and Streitwieser, Jr. A., *Proc. Natl. Acad. Sci. USA*, **79**, 3922(1982).
17. Kos, A.J., Jemmis, E.D., Schleyer, P.v.R., Gleiter, R. and Fishbach, U., *J. Am. Chem. Soc.* **103**, 4996(1981).
18. Schleyer, P.v.R., Kos, A.J. and Kaufmann, E.J., *J. Am. Chem. Soc.* **105**, 7617(1983).
19. Jemmis, E.D., Schleyer, P.v.R. and Pople, J.A., *J. Organomet. Chem.* **154**, 327(1978).
20. Kos, A.J., Poppinger, D. and Schleyer, P.v.R., *Tetrahedron Lett.* **21**, 2151 (1980).
21. Clark, T. and Schleyer, P.v.R., *J. Am. Chem. Soc.* **101**, 7747(1980).
22. Rauscher, G., Clark, T., Poppinger, D. and Schleyer, P.v.R., *Angew. Chem.* **90**, 306(1978).
23. Chandrasekhar, J., Pople, J.A., Seeger, R., Seeger, U. and Schleyer, P.v.R., *J. Am. Chem. Soc.* **104**, 3651(1982).
24. Apeloig, Y., Schleyer, P.v.R. and Pople, J.A., *ibid.* **99**, 1291(1977).
25. Spitznagel, G.W., Clark, T., Chandrasekhar, J. and Schleyer, P.v.R., *J. Comput. Chem.* **3**, 363(1982).
26. Jemmis, E.D., Chandrasekhar, J., Wurthwein, E.-U., Schleyer, P.v.R., Chin, J.W., Landro, F.J., Lagow, R.J. and Pople, J.A., *J. Am. Chem. Soc.* **104**, 4275(1982).
27. Schleyer, P.v.R., Tidor, B., Jemmis, E.D., Chandrasekhar, J., Wurthwein, E.-U., Kos, A.J., Luke, B.T. and Pople, J.A., *ibid.* **105** 484(1983).
28. Schleyer, P.v.R., Wurthwein, E.-U., Kaufmann, E., Clark, T. and Pople, J.A., *J. Am. Chem. Soc.* **105**, 5930(1983).
29. Schleyer, P.v.R., in "New Horizons of Quantum Chemistry", Lowdin, P.-O. and Pullman, A., Eds., Reidel, 1983, p.95.
30. Schleyer, P.v.R., Wurthwein, E.-U. and Pople, J.A., *J. Am. Chem. Soc.* **104**, 5839(1982).

31. Ritchie, J.P., *Tetrahedron Lett.*, **23**, 4999(1982).
32. Reed, A.E. and Weinhold, F., *J. Am. Chem. Soc.* **107**, 1919(1985).
33. Jaworski, A., Person, W.B., Adamowicz, L. and Bartlett, R.J., *Inter. J. Quantum Chem., Quantum Chem. Symp.*, **21**, 613(1987).
34. A series papers making the 100th anniversary of the van't Hoff-Le Bel hypothesis may be found in: Van't Hoff-Le Bel Centennial, O.B.Ramsay, Ed., ACS Symposium Series, no. 12, American Chemical Society, Washington, D.C., 1975.
35. Hartree, D.R., *Proc. Cambridge Phil. Soc.* **24**, 89(1928).
36. Fock, V., *Z. Physik* **61**, 126(1930).
37. Hartree, D.R., Hartree, W. and Swirles, B., *Phil. Transa. Roy. Soc. (London)* **A238**, 229(1939).
38. Roothaan, C.C.J., *Rev. Mod. Phys.* **23**, 69(1951).
39. Pople, J.A. and Nesbet, R.K., *J. Chem. Phys.* **22**, 571(1954).
40. Roothaan, C.C.J., *Rev. Mod. Phys.* **32**, 179(1960).
41. Roothaan, C.C.J. and Bagus, P.S., *Methods in Comput. Phys.* **2**, 47(1963).
42. Pilar, F.L., "*Elementary Quantum Chemistry*", McGraw-Hill Inc., 1968.
43. Ahlrichs, R., Kutzelnigg, W. and Bingel, W.A., *Theoret. Chim. Acta* **5**, 289, 305(1966).
44. Ahlrichs, R. and Kutzelnigg, W., *J. Chem. Phys.* **48**, 1819(1968).
45. Allen, L.C., *Ann. Rev. Phys. Chem.* **20**, 315(1969).
46. Amdur, I. and Jordan, J.E., *Advan. Chem. Phys.* **10**, 29(1966).
47. Aung, S., Pitzer, R.M. and Chan, S.I., *J. Chem. Phys.* **49**, 882(1968).
48. Wahl, A.C. and Das, G., in "*Methods of Electronic Structure Theory*", Schaefer III, H.F., Ed., Plenum, New York, 1977, p.51.
49. Schavitt, I., *ibid.* p.189.
50. Davidson, E.R., "*Proceedings of The First International Congress on Quantum Chemistry*", Daudel, R. and Pullman, B., Eds., Dordrecht, 1974.

51. Szabo, A. and Ostlund, N.S., "*Introduction to Advanced Electronic Structure Theory*", MacMillan Publishing Co., New York, 1982.
52. Hehre, W.J., Radon, L., Schleyer, P.v.R. and Pople, J.A., "*Ab Initio Molecular Orbital Theory*", John Wiley and Sons, Inc., New York, 1986.
53. Siegbahn, P.E.M., Heiberg, A., Roos, B.O. and Levy, B., *Phys. Scr.* **21**, 323(1980).
54. Roos, B.O., Taylor, P.R. and Siegbahn, P.E.M., *Chem. Phys.*, **48**, 157(1980).
55. Siegbahn, P.E.M., Almlof, J., Heiberg, A. and Roos, B.O., *J. Chem. Phys.* **74**, 2384(1981).
56. Born, M. and Oppenheimer, J.R., *Ann. Physik* **84**, 457(1927).
57. Slater, J.C., *Phys. Rev.* **35**, 210(1930).
58. Hylleraas, E.A., *Z. Physik* **48**, 469(1928).
59. Shavitt, I., *Inter. J. Quantum Chem. Symp.* **11**, 133(1977).
60. Olsen, J., Yeager, D.L. and Jorgensen, P., *Advan. Chem. Phys.* **54**, 1(1983).
61. Dalgaard, E. and Jorgensen, P., *J. Chem. Phys.* **69**, 3833(1978).
62. Yeager, D.L. and Jorgensen, P., *J. Chem. Phys.* **71**, 755(1979).
63. Dalgaard, E., *Chem. Phys. Lett.* **65**, 559(1979).
64. Moller, C. and Plesset, M.S., *Phys. Rev.* **46**, 618(1934).
65. Hehre, W.J., Stewart, R.F. and Pople, J.A., *J. Chem. Phys.* **51**, 2657(1969).
66. Hehre, W.J., Ditchfield, R., Stewart, R.F. and Pople, J.A., *ibid.* **52**, 2769(1970).
67. Ditchfield, R., Hehre, W.J. and Pople, J.A., *ibid.* **54**, 724(1971).
68. Hehre, W.J., Ditchfield, R. and Pople, J.A., *ibid.* **56**, 2257(1972).
69. Dill, J.D. and Pople, J.A., *ibid.* **62**, 2921(1975).
70. Hariharan, P.C. and Pople, J.A., *Theoret. Chim. Acta* **28**, 213(1973).
71. Francl, M.M., Pietro, W.J., Hehre, W.J., Binkley, J.S., Gordon, M.S., Defrees, D.J. and Pople, J.A., *J. Chem. Phys.* **77**, 3654(1982).

72. Huzinaga, S., Andzelm, J., Klobukowski, M., Radzio-Andzelm, E., Sakai, Y. and Tatewaki, H., "*Gaussian Basis Sets For Molecular Calculations*", Elsevier, Amsterdam, 1984.
73. Dunning, T.H., Jr., Hay, P.J., in "*Methods of Electronic Structure Theory*", Schaefer III, H.F., Ed. Plenum Press, New York, 1977, P.1.
74. Frisch, M.J., Binkley, J.S., Schlegel, H.B., Raghavachari, K., Melius, C.F., Martin, L., Stewart, J.J.P., Bobrowicz, F.W., Roglfing, C.M., Kahn, L.R., Defrees, D.J., Seeger, R., Whiteside, R.A., Fox, D.J., Fleuder, E.M. and Pople, J.A., *GAUSSIAN86* ReleaseC, Carnegie-Mellon University, 1987.
75. Pople, J.A. and Gordon, M.S., *J. Am. Chem. Soc.* **89**, 4253(1967).
76. Mulliken, R.S., *J. Chem. Phys.* **23**, 1833, 1841, 2338, 2343(1955).
77. Collins, J.B. and Streitwieser, A., Jr. *J. Comput. Chem.* **1**, 81(1980).
78. Disch, R.L., Schulman, J.M. and Ritchie, J.P., *J. Am. Chem. Soc.* **106**, 6246(1984).